Table 2. Patients' characteristics

No.	Group (courses of treatments)	Age	Sex	KPS	Stage (metastasis)	Comment
1	Naive	50	M	90	Locally advanced	The third injection of the first course was omitted by high fever
2	Naive	57	M	90	Locally advanced	
3	Treated (3)	74	F	100	Locally advanced	The third course was irregular by patient's private matter
4	Treated (4)	76	M	90	Locally advanced	The second course was irregular by pancreatitis
5	Treated (20)	70	F	90	Metastasis (HEP)	
6	Treated (9)	56	M	100	Locally advanced	The second injection of the second course was omitted by high fever
7	Naive	62	F	90	Metastasis (HEP, SPL)	
8	Naive	81	M	90	Locally advanced	
9	Treated (3)	68	F	90	Locally advanced	
10	Treated (5)	70	M	100	Locally advanced	
11	Naive	74	F	100	Metastasis (PUL)	The third course was irregular by nausea
12	Treated (12)	72	M	100	Metastasis (PER)	
13	Treated (9)	54	F	100	Metastasis (HEP)	
14	Naive	70	M	100	Metastasis (PUL, PLE)	Terminated by PD in the second course
15	Naive	57	F	80	Metastasis (PLE, OSS)	Terminated by pneumonia in the first course
16	Treated (8)	64	M	90	Locally advanced	
17	Treated (5)	78	F	90	Metastasis (PER)	
18	Naive	56	F	90	Locally advanced	
19	Naive	48	M	90	Locally advanced	
20	Naive	80	M	100	Locally advanced	
21	Naive	59	F	80	Metastasis (HEP)	Terminated by PD in the second course
22	Naive	65	F	90	Locally advanced	The second injection of the second course was omitted by high fever
23	Naive	52	M	90	Locally advanced	The first course was irregular by neutropenia
24	Naive	78	F	90	Locally advanced	
25	Naive	65	F	100	Metastasis (HEP)	
26	Naive	80	F	100	Metastasis (LN)	
27	Naive	82	F	100	Metastasis (PER, LN)	
28	Naive	71	F	90	Metastasis (PUL)	The second injection of the second course was omitted by patient's private matter

KPS, Karnofsky performance score; HEP, liver; SPL, spleen; PUL, lung; PER, peritoneum; PLE, pleura; OSS, bone; LN, lymph node; PD, progressive disease.

(Fig. 2F), $CD69^+CD4^+$ T cells ($P = 0.048$) (Fig. 2L) and $CD69^+CD8^+$ T cells ($P = 0.015$) (Fig. 2M) decreased on day 14. $CD8^+$ T cells ($P = 0.010$ and $P = 0.030$) and memory CD4 lymphocytes ($P = 0.020$ and $P = 0.010$) took 2 months to recover (Fig. 2E and K). B cells ($P = 0.022$, $P = 0.011$ and $P = 0.005$, Fig. 2H) and NKT cells ($P = 0.035$, $P = 0.042$ and $P = 0.013$, Fig. 2G) did not recover during the 2 months of the monitoring period. $CD123^+$ DC increased before the second course ($P = 0.017$), and there was no significant difference between the third course (Fig. 2P). Only $CD11c^+$ DC showed a constant increase over 2 months ($P = 0.011$ and $P = 0.021$, Fig. 2Q). $CD14^+$ monocytes temporarily decreased at day 14, but returned to the pre-treatment count before the third course of treatment ($P = 0.033$, Fig. 2I).

Pentamer Analysis

The percentage of CMV-specific T cell was examined in seven patients in the naive group and four in the treated group (Supplementary Fig. S2). The percentage of CMV-positive cells was not different between the naive and treated groups (Supplementary Fig. S2A). A subtype analysis was performed in Patient no. 27 and there were no changes in the percentages of naive ($CD8^+CD27^+CD45RA^+$), memory ($CD8^+CD45RA^-$), effector ($CD8^+CD27^-CD45RA^+$) and central memory cells ($CD8^+CD57^-CD45RO^+$) (Supplementary Fig. S2B). Hence, gemcitabine treatment did not affect CMV-specific T cells. WT1-specific T cells were examined by a pentamer analysis in 5 patients with HLA-A02, 10 patients with HLA-A24 and

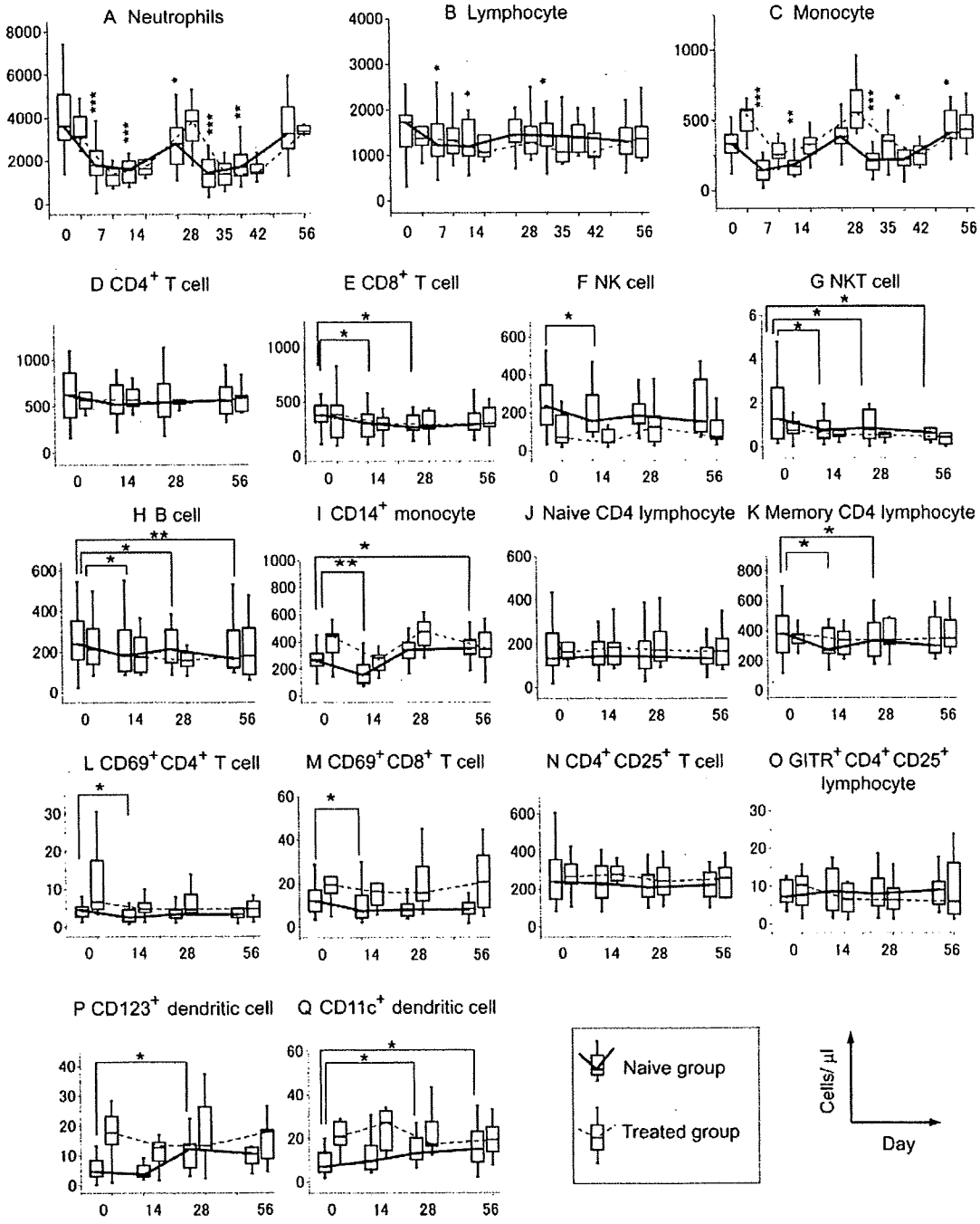

Figure 2. Kinetic of absolute numbers of immune cells during gemcitabine treatment. $CD69^+CD4^+$ T cell (L), D69 $CD8^+$ T cell (M), $CD14^+$ monocyte (I), $CD123^+$ dendritic cell (P) and $CD11c^+$ dendritic cell (Q) increased in the treated group. $CD14^+$ monocyte (I), $CD123^-$ dendritic cell (P) and $CD11c^+$ dendritic cell (Q) increased gradually, following gemcitabine treatment in the naive group. Significant difference between pre-treatment and post-treatment samples in the naive group: *, ** and *** indicates $P < 0.050$, $P < 0.010$ and $P < 0.001$, respectively. P value of the naive group vs. the treated group by repeated measured design. A, $P = 0.444$; B, $P = 0.753$; C, $P = 0.001$; D, $P = 0.572$; E, $P = 0.791$; F, $P = 0.072$; G, $P = 0.166$; H, $P = 0.099$; I, $P = 0.021$; J, $P = 0.663$; K, $P = 0.838$; L, $P = 0.002$; M, $P = 0.012$; N, $P = 0.551$; O, $P = 0.433$; P, $P < 0.001$; Q, $P < 0.001$.

6 patients with HLA-A02/A24 (Supplementary Fig. S2C). The frequency of WT1 pentamer-positive cells in HLA-A24 cells tended to be higher than that in HLA-A02. However, HLA-A2402 WT1 pentamer-positive cells did not make cluster patterns and were considered as non-specific binding.

Intracellular Cytokine Analysis and T Cell Repertoire Analysis

The absolute numbers and percentages of IL-4- and IFN-γ-producing T cells in $CD8^+$ and $CD4^+$ T cells were analyzed (Fig. 3 and Supplementary Fig. S3). Gemcitabine

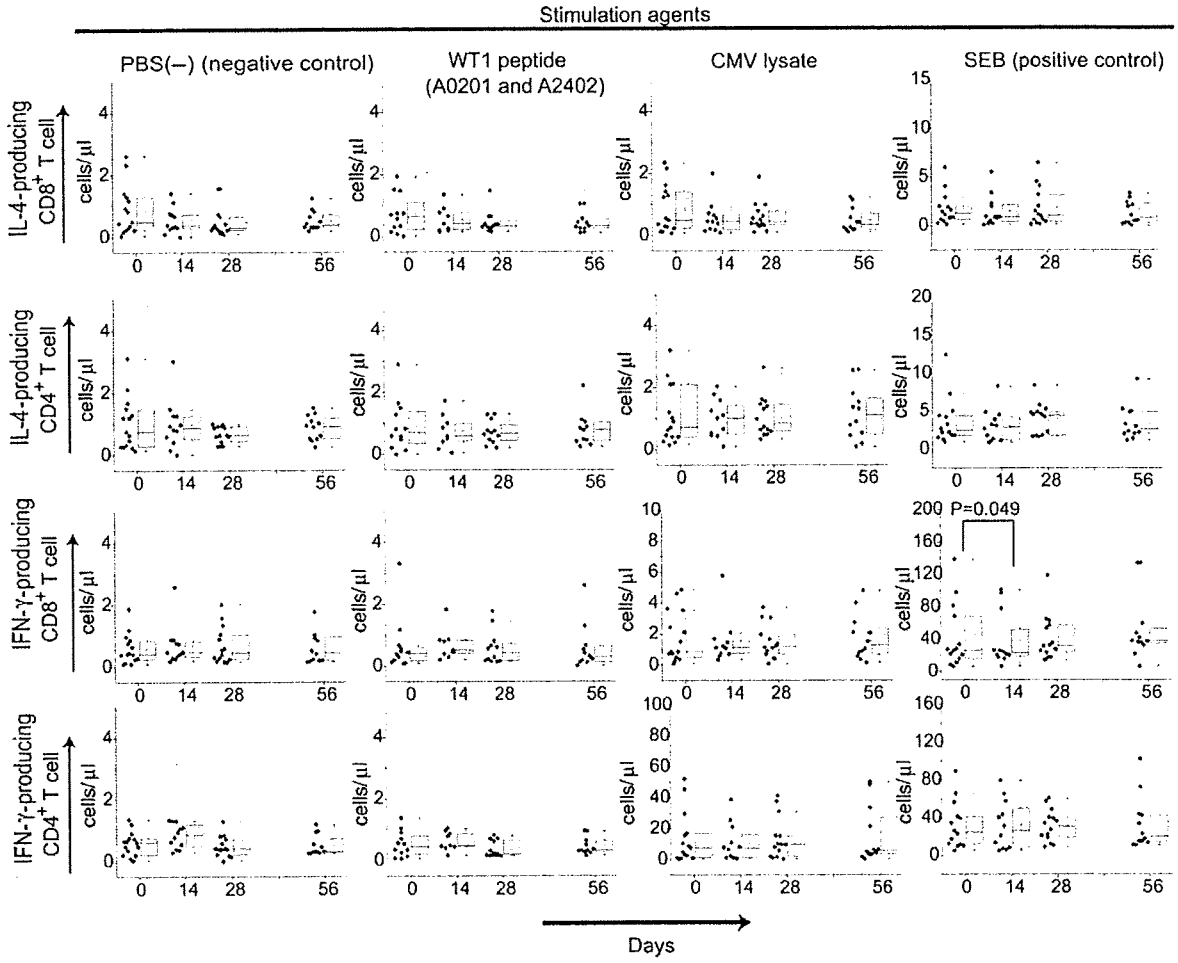

Figure 3. Kinetic of the absolute number of cytokine-producing cells during gemcitabine treatment. Cytokine production stimulated with WT1 peptides, CMV lysate or SEB was not influenced by gemcitabine treatment, except for interferon (IFN)-γ production of $CD8^+$ T cell stimulated with SEB.

treatment only influenced the absolute number of IFN-γ-producing $CD3^+CD8^+$ lymphocytes as determined by staphylococcal enterotoxin B (SEB) stimulation (on day 14, $P = 0.049$). The level of cytokine production inducted by WT1-peptide stimulation was same as PBS(−) (negative control). A simple regression analysis revealed a strong correlation between them ($R = 0.66799–0.88675$) and suggested that compensation by subtracting the percentage of negative control is needed to detect actual reactivation with WT1 peptide. Figure 4 shows the compensated percentage of cytokine-producing cells. The compensated percentage of IL-4- and IFN-γ-producing cells induced by WT1-peptide stimulation was <0.3%, suggesting that WT1 peptides had almost no effects for cytokine production in this study. The difference in percentage of IL-4-producing cells induced by CMV lysate or SEB was statistically significant between pre-treatment and post-treatment; however, the change of the percentage was very small and considered to be of little importance.

T cell repertoire analysis was performed in five patients in the naive group. The size distribution of TCR did not show any significant change which suggests that gemcitabine does not affect the T cell repertoire.

DISCUSSION

As our knowledge of cellular and molecular immunology has increased, the mechanism of anticancer immunity has been explored and many tumor-associated antigens have been identified, which has contributed to the recent development of cancer vaccine trials. Although prophylactic cancer vaccine against cervical cancers (GARDASIL®, CERVARIX®) has already been approved in several countries, clinical trials of therapeutic cancer vaccines have shown only limited efficacy (12). To improve the efficacy of therapeutic cancer vaccines, several approaches have been tried. One strategy is to give such vaccines to patients with minimal residual disease (13), and another is to give vaccines in combination with chemotherapeutic agents and/or radiotherapy to temporarily control cancer growth and/or to

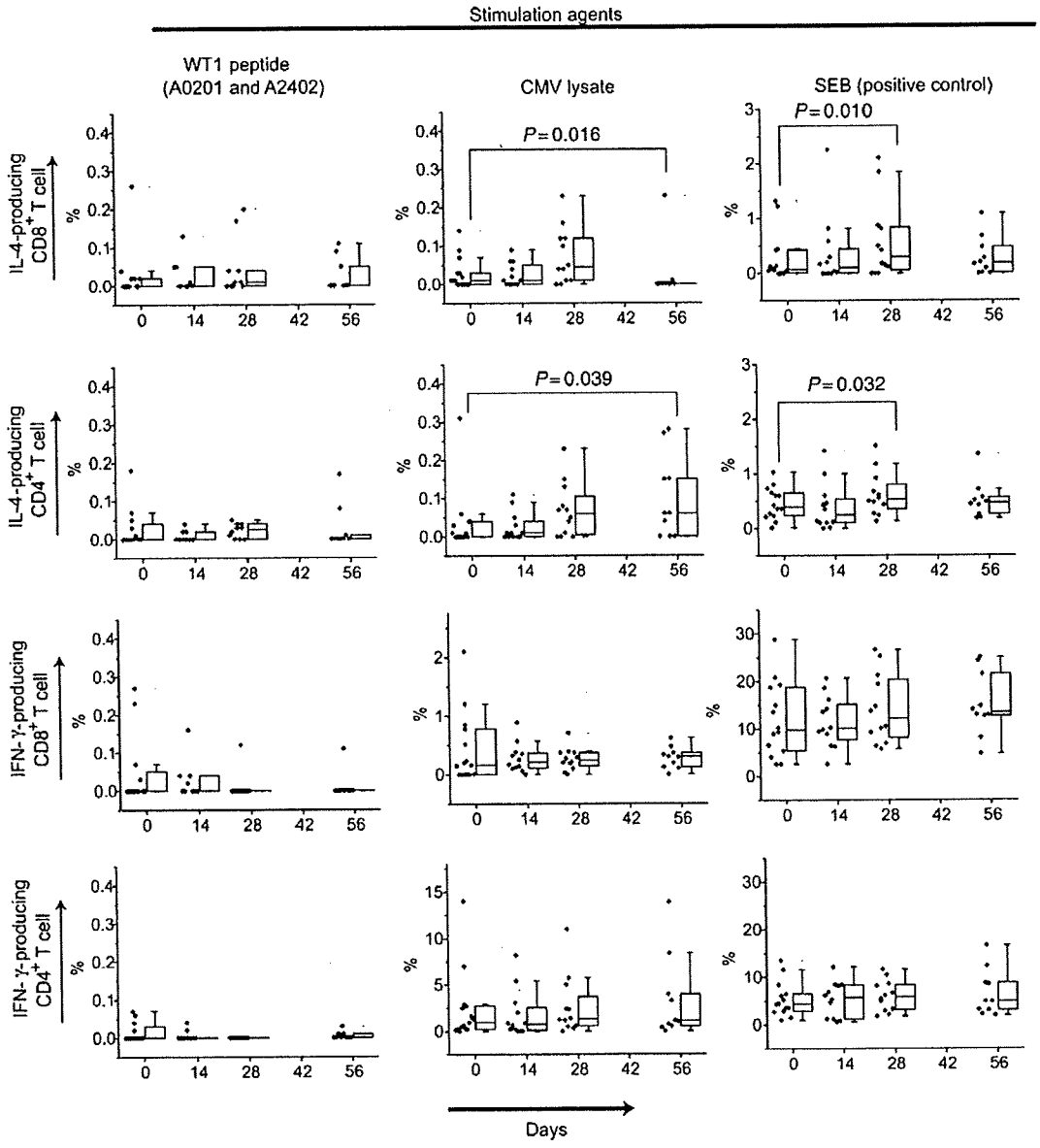

Figure 4. The compensated percentage of cytokine-producing cells in each T cell subtype. The percentage of interleukin (IL)-4- and IFN-γ-producing cells was <0.3% by WT1-peptide stimulation. The difference in IL-4 production stimulated by CMV lysate and SEB was statistically significant; however, the change was very small.

achieve synergistic effects (14,15). It is well known that many cytotoxic drugs induce an immunosuppressive status and some of them are actually used as immunosuppressants for the treatment of autoimmune diseases and as post-transplantation prophylaxis for graft-versus-host disease. On the other hand, it was recently revealed that some chemotherapeutic agents induce positive immunological reactions. Cyclophosphamide enhanced anti-tumor immunity by reducing the immunosuppressive effects of $CD4^+CD25^+$ regulatory T cells (16). Oxaliplatin and doxorubicin also enhance immunity by injuring tumor cells to release HMGB1 protein, which is a ligand of Toll-like receptor-4 that activates DC (17). Cytotoxic agents including cisplatin, doxorubicin, mitomycin C, fluorouracil and camptothecin induce the apoptosis of cancer cells via Fas or TRAIL-dependent pathways (18,19).

Gemcitabine has multiple immunostimulatory effects. It enhances antigen presentation by inducing tumor apoptosis (20,21) and eliminates myeloid-derived suppressor cells (22). It was also reported that gemcitabine treatment inhibited B-cell proliferation and the production of anti-influenza virus antibody in a mouse model (23). Nowak et al. (24) reported that gemcitabine and CD40L had synergistic effects toward solid tumors. Bauer et al. (25) also showed that combination therapy with gemcitabine and DC-based vaccination had higher efficacy in a Panc02 pancreatic tumor cell line.

Furthermore, Correale et al. (26) reported the results of a clinical trial of chemo-immunotherapy against colon cancer with gemcitabine plus FOLFOX4 followed by granulocyte-macrophage colony-stimulating factor and IL-2. They showed an increase in the expression of tumor-associated antigen (carcinoembryonic antigen and thymidylate synthase) and a suppression of regulatory T cells. However, the mechanism by which gemcitabine affects the immune system is not yet fully elucidated. The results of immunological monitoring in pancreatic cancer patients were reported by Plate et al. (9) who concluded that gemcitabine therapy was not immunosuppressive and may actually enhance the response to vaccine by reducing $CD3^+CD45RO^+$ memory T cells. However, their study encompassed a shorter period of only 21 days, and the gemcitabine treatment schedule was different from ours. Bang et al. (27) reported an increase in $CD11c^+$ myeloid DC under combination therapy with gemcitabine and cisplatin.

In this study, we evaluated the immunological effects of gemcitabine as a single agent over a 2-month period in pancreatic cancer patients. Our results showed that the decreases in T lymphocytes and NK cells were transient, and gemcitabine treatment increased CD14+ monocytes and two types of DC. We showed that conventional gemcitabine treatment increased the number of antigen-presenting cells (APCs). In cancer patients, it has been reported that levels of circulating DC were lower than those in healthy individuals (28) and the differentiation of DC was inhibited by tumor cells (29,30). Our result indicated that gemcitabine may act on APC both locally and systemically in a clinical setting. This reaction may activate innate immunity and then stimulate the acquired immune system via activated APC, and finally induce tumor cell death. These effects of gemcitabine on APCs may be an advantage of combination therapy with cancer vaccine.

Previously, we reported that the appearance of WT1-specific T lymphocytes after allogeneic hematopoietic stem cell transplantation correlated with the development of graft-versus-host disease and the clinical response for malignant diseases (31). WT1 protein is found in leukemia (32), breast cancer (33) and many solid cancer cell lines (34), and clinical trials of WT1-peptide vaccine have already been started by several groups (35,36). Pancreatic cancer also expresses WT1 protein in 75% of the cases (37). Antigen-specific T cells and IFN-producing function were not affected by gemcitabine treatment. All of these results suggest that the combination of gemcitabine and WT1-peptide vaccine could be a suitable chemo-immunotherapy against pancreatic cancers.

Our study also demonstrated several limitations to establish the proof of concept in our future WT1-peptide therapy. In WT1-specific pentamer analysis, the specificity of HLA-A0201-restricted pentamer appears to be a useful tool for evaluating WT1-specific cytotoxic T lymphocyte. However, HLA-A2402 pentamer showed non-specific binding potential to CD8-negative T lymphocytes, which results in a wide distribution of CD8-positive/negative cells. None of the samples clearly secreted INF-γ after HLA-A2402 peptide stimulation, even if they contained pentamer-positive cells. Even though the patients in the gemcitabine naive and treated groups had almost the same backgrounds, several patients in the naive group discontinued gemcitabine treatment, which suggests that the two groups actually reflect different populations. Indeed, progression-free survival in the naive and treated groups was 6 vs. 20.6 months ($P < 0.001$). Nevertheless, our results may still suggest that combination therapy consisting of gemcitabine and WT1-peptide vaccine may become a novel chemo-immunotherapy against advanced pancreatic cancer.

Supplementary data

Supplementary data are available at http://www.jjco.oxfordjournals.org.

Funding

This study was supported by Grants in Aid for Cancer Research from Ministry of Health, Labour and Welfare of Japan.

Conflict of interest statement

None declared.

References

1. Ministry of Health, Labour and Welfare. Abridged Life Table for Japan 2006. http://www.mhlw.go.jp/toukei/saikin/hw/jinkou/kakutei06/hyo7.html (1 December 2008, date last accessed).
2. Jemal A, Siegel R, Ward E, Murray T, Xu J, Thun MJ. Cancer statistics. *CA Cancer J Clin* 2007;57:43–66.
3. Burris HA, Moore MJ, Andersen J, Green MR, Rothenberg ML, Modiano MR, et al. Improvements in survival and clinical benefit with gemcitabine as first-line therapy for patients with advanced pancreas cancer: a randomized trial. *J Clin Oncol* 1997;15:2403–13.
4. Berlin JD, Catalano P, Thomas JP, Kugler JW, Haller DG, Benson AB. Phase III study of gemcitabine in combination with fluorouracil versus gemcitabine alone in patients with advanced pancreatic carcinoma: Eastern Cooperative Oncology Group Trial E2297. *J Clin Oncol* 2002;20:3270–5.
5. Louvet C, Labianca R, Hammel P, Lledo G, Zampino MG, Andre T, et al. Gemcitabine in combination with oxaliplatin compared with gemcitabine alone in locally advanced or metastatic pancreatic cancer: results of a GERCOR and GISCAD phase III trial. *J Clin Oncol* 2005;23:3509–16.
6. Oettle H, Richards D, Ramanathan RK, van Leathem JL, Peeters M, Fuchs M, et al. A phase III trial of pemetrexed plus gemcitabine versus gemcitabine in patients with unresectable or metastatic pancreatic cancer. *Ann Oncol* 2005;16:1639–45.
7. Van Cutsem E, van de Velde H, Karasek P, Oettle H, Vervenne WL, Szawlowski A, et al. Phase III trial of gemcitabine plus tipifarnib compared with gemcitabine plus placebo in advanced pancreatic cancer. *J Clin Oncol* 2004;22:1430–8.
8. Moore MJ, Goldstein D, Hamm J, Figer A, Hecht JR, Gallinger S, et al. Erlotinib plus gemcitabine compared with gemcitabine alone in patients with advanced pancreatic cancer: a phase III trial of the National

Cancer Institute of Canada Clinical Trials Group. *J Clin Oncol* 2007;25:1960–6.
9. Plate JM, Plate AE, Shott S, Bograd S, Harris JE. Effect of gemcitabine on immune cells in subjects with adenocarcinoma of the pancreas. *Cancer Immunol Immunother* 2005;54:915–25.
10. Choi YW, Kotzin B, Herron L, Callahan J, Marrack P, Kappler J. Interaction of *Staphylococcus aureus* toxin 'superantigens' with human T cells. *Proc Natl Acad Sci USA* 1989;86:8941–5.
11. Labrecque N, McGrath H, Subramanyam M, Huber BT, Sekaly RP. Human T cells respond to mouse mammary tumor virus-encoded superantigen: V beta restriction and conserved evolutionary features. *J Exp Med* 1993;177:1735–43.
12. Rosenberg SA, Yang JC, Restifo NP. Cancer immunotherapy: moving beyond current vaccines. *Nat Med* 2004;10:909–15.
13. Hoos A, Parmiani G, Hege K. A clinical development paradigm for cancer vaccines and related biologics. *J Immunother* 2007;30:1–15.
14. Menard C, Martin F, Apetoh L, Bouyer F, Ghiringhelli F. Cancer chemotherapy: not only a direct cytotoxic effect, but also an adjuvant for antitumor immunity. *Cancer Immunol Immunother* 2008;57: 1579–87.
15. Zitvogel L, Apetoh L, Ghiringhelli F, Kroemer G. Immunological aspects of cancer chemotherapy. *Nat Rev Immunol* 2008;8:59–73.
16. Ghiringhelli F, Menard C, Puig PE, Ladoire S, Roux S, Martin F, et al. Metronomic cyclophosphamide regimen selectively depletes $CD4^+CD25^+$ regulatory T cells and restores T and NK effector functions in end stage cancer patients. *Cancer Immunol Immunother* 2007;56:641–8.
17. Apetoh L, Ghiringhelli F, Tesniere A, Obeid M, Ortiz C, Criollo A, et al. Toll-like receptor 4-dependent contribution of the immune system to anticancer chemotherapy and radiotherapy. *Nat Med* 2007;13: 1050–9.
18. Lacour S, Hammann A, Wotawa A, Corcos L, Solary E, Dimanche-Boitrel MT. Anticancer agents sensitize tumor cells to tumor necrosis factor-related apoptosis-inducing ligand-mediated caspase-8 activation and apoptosis. *Cancer Res* 2001;61:1645–51.
19. Micheau O, Solary E, Hammann A, Martin F, Dimanche-Boitrel MT. Sensitization of cancer cells treated with cytotoxic drugs to fas-mediated cytotoxicity. *J Natl Cancer Inst* 1997;89:783–9.
20. Zisman A, Ng CP, Pantuck AJ, Bonavida B, Belldegrun AS. Actinomycin D and gemcitabine synergistically sensitize androgen-independent prostate cancer cells to Apo2L/TRAIL-mediated apoptosis. *J Immunother* 2001;24:459–71.
21. Correale P, Cusi MG, Del Vecchio MT, Aquino A, Prete SP, Tsang KY, et al. Dendritic cell-mediated cross-presentation of antigens derived from colon carcinoma cells exposed to a highly cytotoxic multidrug regimen with gemcitabine, oxaliplatin, 5-fluorouracil, and leucovorin, elicits a powerful human antigen-specific CTL response with antitumor activity in vitro. *J Immunol* 2005;175:820–8.
22. Suzuki E, Kapoor V, Jassar AS, Kaiser LR, Albelda SM. Gemcitabine selectively eliminates splenic Gr-1+/CD11b+ myeloid suppressor cells in tumor-bearing animals and enhances antitumor immune activity. *Clin Cancer Res* 2005;11:6713–21.
23. Nowak AK, Robinson BW, Lake RA. Gemcitabine exerts a selective effect on the humoral immune response: implications for combination chemo-immunotherapy. *Cancer Res* 2002;62:2353–58.
24. Nowak AK, Robinson BW, Lake RA. Synergy between chemotherapy and immunotherapy in the treatment of established murine solid tumors. *Cancer Res* 2003;63:4490–6.
25. Bauer CA, Bauernfeind F, Sterzik A, Orban M, Schnurr M, Lehr HA, et al. Dendritic cell-based vaccination combined with gemcitabine increases survival in a murine pancreatic carcinoma model. *Gut* 2007;56:1275–82.
26. Correale P, Cusi MG, Tsang KY, Del Vecchio MT, Marsili S, Placa ML, et al. Chemo-immunotherapy of metastatic colorectal carcinoma with gemcitabine plus FOLFOX 4 followed by subcutaneous granulocyte macrophage colony-stimulating factor and interleukin-2 induces strong immunologic and antitumor activity in metastatic colon cancer patients. *J Clin Oncol* 2005;23:8950–8.
27. Bang S, Kim HS, Choo YS, Park SW, Chung JB, Song SY. Differences in immune cells engaged in cell-mediated immunity after chemotherapy for far advanced pancreatic cancer. *Pancreas* 2006;32:29–36.
28. Almand B, Resser JR, Lindman B, Nadaf S, Clark JI, Kwon ED, et al. Clinical significance of defective dendritic cell differentiation in cancer. *Clin Cancer Res* 2000;6:1755–66.
29. Oyama T, Ran S, Ishida T, Nadaf S, Kerr L, Carbone DP, et al. Vascular endothelial growth factor affects dendritic cell maturation through the inhibition of nuclear factor-kappa B activation in hemopoietic progenitor cells. *J Immunol* 1998;160:1224–32.
30. Gabrilovich DI, Chen HL, Girgis KR, Cunningham HT, Meny GM, Nadaf S, et al. Production of vascular endothelial growth factor by human tumors inhibits the functional maturation of dendritic cells. *Nat Med* 1996;2:1096–103.
31. Morita Y, Heike Y, Kawakami M, Miura O, Nakatsuka S, Ebisawa M, et al. Monitoring of WT1-specific cytotoxic T lymphocytes after allogeneic hematopoietic stem cell transplantation. *Int J Cancer* 2006;119:1360–7.
32. Inoue K, Sugiyama H, Ogawa H, Nakagawa M, Yamagami T, Miwa H, et al. WT1 as a new prognostic factor and a new marker for the detection of minimal residual disease in acute leukemia. *Blood* 1994;84:3071–9.
33. Loeb DM, Evron E, Patel CB, Sharma PM, Niranjan B, Buluwela L, et al. Wilms' tumor suppressor gene (WT1) is expressed in primary breast tumors despite tumor-specific promoter methylation. *Cancer Res* 2001;61:921–5.
34. Oji Y, Ogawa H, Tamaki H, Oka Y, Tsuboi A, Kim EH, et al. Expression of the Wilms' tumor gene WT1 in solid tumors and its involvement in tumor cell growth. *Jpn J Cancer Res* 1999;90:194–204.
35. Morita S, Oka Y, Tsuboi A, Kawakami M, Maruno M, Izumoto S, et al. A phase I/II trial of a WT1 (Wilms' tumor gene) peptide vaccine in patients with solid malignancy: safety assessment based on the phase I data. *Jpn J Clin Oncol* 2006;36:231–6.
36. Oka Y, Tsuboi A, Taguchi T, Osaki T, Kyo T, Nakajima H, et al. Induction of WT1 (Wilms' tumor gene)-specific cytotoxic T lymphocytes by WT1 peptide vaccine and the resultant cancer regression. *Proc Natl Acad Sci USA* 2004;101:13885–90.
37. Oji Y, Nakamori S, Fujikawa M, Nakatsuka S, Yokota A, Tatsumi N, et al. Overexpression of the Wilms' tumor gene WT1 in pancreatic ductal adenocarcinoma. *Cancer Sci* 2004;95:583–7.

The Pharmacogenomics Journal (2009) 9, 137–146

www.nature.com/tpj

ORIGINAL ARTICLE

A new statistical screening approach for finding pharmacokinetics-related genes in genome-wide studies

Y Sato[1,2], NM Laird[1], K Nagashima[3], R Kato[3], T Hamano[4], A Yafune[5], N Kaniwa[6,7], Y Saito[6,8], E Sugiyama[6,7], S-R Kim[6], J Furuse[9], H Ishii[9], H Ueno[10], T Okusaka[10], N Saijo[11], J-i Sawada[6,8] and T Yoshida[2]

[1]*Department of Biostatistics, Harvard School of Public Health, Boston, MA, USA;* [2]*Genetics Division, National Cancer Center Research Institute, Tokyo, Japan;* [3]*Faculty of Engineering, Tokyo University of Science, Tokyo, Japan;* [4]*Hamano Statistical Analysis Ltd., Tokyo, Japan;* [5]*Clinic Sendagaya, Tokyo, Japan;* [6]*Project Team for Pharmacogenetics, National Institute of Health Sciences, Tokyo, Japan;* [7]*Division of Medicinal Safety Science, National Institute of Health Sciences, Tokyo, Japan;* [8]*Division of Functional Biochemistry and Genomics, National Institute of Health Sciences, Tokyo, Japan;* [9]*Hepatobiliary and Pancreatic Oncology Division, National Cancer Center Hospital East, Chiba, Japan;* [10]*Hepatobiliary and Pancreatic Oncology Division, National Cancer Center Hospital, Tokyo, Japan and* [11]*National Cancer Center Hospital East, Chiba, Japan*

Correspondence:
Dr T Yoshida, Genetics Division, National Cancer Center Research Institute, 5-1-1 Tsukiji, Chuo-ku, Tokyo 104-0045, Japan.
E-mail: tyoshida@ncc.go.jp

Received 7 August 2008; revised 11 November 2008; accepted 19 November 2008; published online 23 December 2008

Biomedical researchers usually test the null hypothesis that there is no difference of the population mean of pharmacokinetics (PK) parameters between genotypes by the Kruskal–Wallis test. Although a monotone increasing pattern with a number of alleles is expected for PK-related genes, the Kruskal–Wallis test does not consider a monotonic response pattern. For detecting such patterns in clinical and toxicological trials, a maximum contrast method has been proposed. We show how that method can be used with pharmacogenomics data to a develop test of association. Further, using simulation studies, we compare the power of the modified maximum contrast method to those of the maximum contrast method and the Kruskal–Wallis test. On the basis of the results of those studies, we suggest rules of thumb for which statistics to use in a given situation. An application of all three methods to an actual genome-wide pharmacogenomics study illustrates the practical relevance of our discussion.
The Pharmacogenomics Journal (2009) **9**, 137–146; doi:10.1038/tpj.2008.17; published online 23 December 2008

Keywords: gemcitabine; genome-wide study; maximum contrast method; pharmacokinetics-related gene; statistical screening method

Introduction

Interindividual variation in drug response among patients is well known and poses a serious problem in medicine. The variation could be because of multiple factors such as disease phenotypes, genetic and environmental factors and the variability in drug target response (pharmacodynamic response) or allergic response, all factors that affect drug absorption, distribution, metabolism and excretion, side effects or efficacy.[1–3] However, at present, few biomarkers can predict, which group of patients will respond positively, which patients are nonresponders and who might experience adverse reactions for the same medication and dose. To realize personalized medicine, it is critically important to observe individual differences in drug response and the role of genetic polymorphisms that are relevant to the pathways of drug metabolism and the biology of drug responses in the pharmacogenomics of common diseases.[4]

With this background, the Food and Drug Administration (FDA) recognizes the importance of pharmacogenomics and has issued a guidance that encourages pharmacogenomics during drug development.[5] Many pharmacogenomics studies have been launched worldwide, such as a combination of a pharmaco-

kinetic (PK) study and analyses of single nucleotide polymorphisms (SNPs) in a candidate gene or in a genome-wide approach. Following the completion of the HapMap project,[6] the advent of the powerful array-based SNP typing platforms has heralded an era in which a genome-wide approach is a popular or standard strategy for identifying disease susceptibility or drug response genes for common diseases.[7–9]

To identify the SNPs, which relate to the pathways of drug metabolism, biomedical researchers usually test the null hypothesis (H_0) that there is no difference of the population mean of PK parameters (that is, area under the curve (AUC), maximum drug concentration (C_{max}), half-life period ($t_{1/2}$) and so on) between genotypes by using mainly the nonparametric analysis of variance, that is, the Kruskal–Wallis test.[10,11] On the basis of the statistical significance of the results from that test, researchers check the PK-genotype response patterns by sight, and then detect an additive, recessive or dominant model. The PK-related genes indicate a monotone increasing pattern in the number of alleles such as genetic models (additive, recessive and dominant pattern) as shown in Figure 1. Because a genome-wide association study is often designed as a multistage process, a relatively relaxed type I error rate is adopted in the first stage screening to assure the overall power of the study. If the Kruskal–Wallis test is applied to a significance level of $P=0.05$ in the first stage of a genome-wide association study, it is expected that as many as 5000–50 000 SNPs should be visually inspected for the current standard genome scan typing platform. Development of more objective and efficient screening method than the current subjective procedure is needed.

As a statistical method for detecting a monotonic dose–response relationship, a maximum contrast method has been proposed in clinical trials and toxicological trials.[12–17] This method, formed by taking the maximum over multiple contrast statistics for detecting a monotonic increase with the dose levels, is useful. The dose–response curves are modeled as the response patterns, and the set of contrast statistics is determined based on the set of contrast coefficients that correspond to these patterns. The contrast statistics should consist of contrast coefficients that are highly correlated with the population means for realistic dose–response relationships. The maximum contrast method is then applied to this set, and the pattern of the contrast coefficients for the contrast statistic that takes the maximum value is then selected as the true response pattern (see Materials and methods section).

In a typical pharmacogenomics study, the association of between PK parameter and genotype is modeled as the response patterns in Figure 1, and then the maximum contrast method is applied to this study on three contrast statistics with the following coefficients: $\boldsymbol{c}_1=(-1\ 0\ 1)^t$, $\boldsymbol{c}_2=(-2\ 1\ 1)^t$, $\boldsymbol{c}_3=(-1\ -1\ 2)^t$. The first contrast statistics corresponds to an additive model, the second to a recessive model and the third to a dominant model. As a result, the pattern of the coefficients for the contrast statistic that takes the maximum value is then selected as the true response pattern. However, the sample size of each genotype was enormously unbalanced, because the minor allele frequency (MAF) is less than 0.5, and the population is in Hardy–Weinberg equilibrium (HWE). Here we propose a modified maximum contrast method to detect an association between a PK parameter and genotype that accounts for the imbalance in genotype groups (see Materials and methods section).

In this paper, we proposed a modified maximum contrast method for detecting an association between PK parameter and genotype. Further, using simulation studies, we compare the Kruskal–Wallis test, the maximum contrast method and the modified maximum contrast method for pharmacogenomics data. We also suggest rules of thumb for

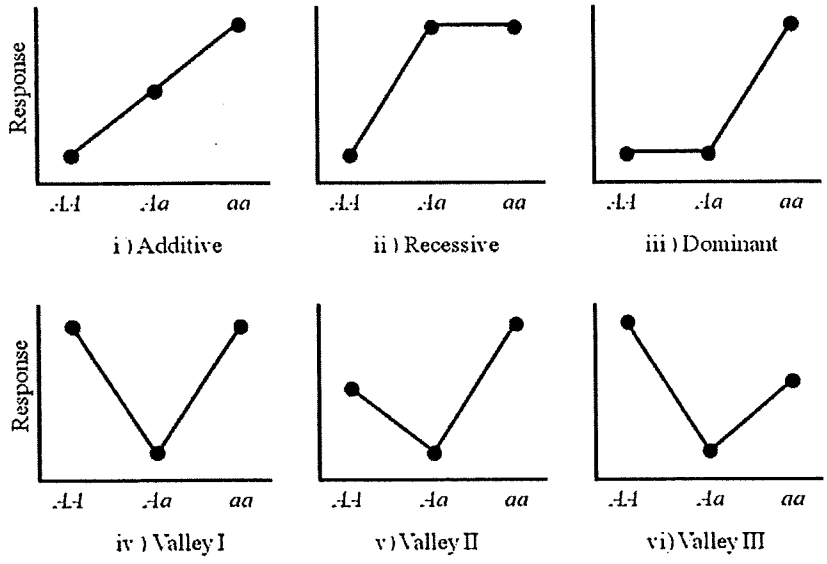

Figure 1 Pharmacokinetics parameter–genotype response patterns.

choosing a powerful maximum contrast statistic for such data. Finally, the discussed methodology is illustrated by its application to a pharmacogenomics study to antitumor drugs on Japanese cancer patients.

Results

Simulation study

To assess the power of the Kruskal–Wallis test, the maximum contrast method and the modified maximum contrast method, we first performed a Monte-Carlo simulation. Summary results of the simulation for each method are shown in Table 1 for various values of Δ and MAF when sample size (n) is set at 300. Note first that the diagonal box shows the positive predictive value (R_{TP}) for detection of true response patterns, whereas the row at the far right is the power (R_p) for detection of PK-related SNPs and includes the misidentification of true response patterns, where the result of R_{TP} by the Kruskal–Wallis test is blank because that test is an overall test and rejects the null hypothesis that there is no difference of the population mean of PK parameters. In a case where $\Delta = 0$, the R_p corresponds to a type I error rate of 5%, and is mostly controlled below 5%, but is inflated slightly for some models. The R_p and R_{TP} increase with increasing Δ; on the other hand, both R_p and R_{TP} decrease as the MAF decreases. We evaluated each method for detecting true response patterns. As a result, when the MAF is less than or equal to 0.25, in the additive and dominant pattern, the modified maximum contrast method is about 0.1–0.4 higher than the maximum contrast method in the R_{TP}. However, in the recessive model, the modified maximum contrast method is about 0.4 lower than the maximum contrast method in the R_{TP}. Therefore, under unbalanced sample size, the modified maximum contrast method is more powerful for detecting true response patterns than the maximum contrast method in the additive and dominant model, whereas the maximum contrast method is more powerful than the modified maximum contrast method in the recessive model.

For detecting PK-related genes, the Kruskal–Wallis test is lower in power than both maximum contrast methods in the R_p, under equivalent sample size (MAF = 0.5), whereas the Kruskal–Wallis test is about 0.05–0.10 higher in power than both maximum contrast methods under the unbalanced sample size (MAF $\leqslant$ 0.25). On the other hand, the R_p of the Kruskal–Wallis test is about 0.10–0.50 higher than both maximum contrast methods under the simulation condition without the PK-related SNPs in Table 2. Therefore the simulation studies suggest that the Kruskal–Wallis test detects many PK-nonrelated SNPs because of not considering the response patterns.

Questionnaire survey on judgment

We next conducted a questionnaire survey to compare the judgment by each statistical method (modified maximum contrast method and maximum contrast method) with the judgment by experts. The results are shown in Table 3. For the recessive and no-response pattern, the judgment of both statistical methods well accords with the judgment by expert. For the additive and dominant pattern, the maximum contrast method detects as a recessive pattern by mistake, and the modified maximum contrast method well accords with the judgment by expert. The Kendall's rank correlation coefficient between modified maximum contrast method and expert's judgment is 0.731; on the other hand, the correlation coefficient between the maximum contrast method and expert's judgment is 0.423. The conclusion is that the judgment of modified maximum contrast method is closer to the judgment by expert than is the maximum contrast method.

Application to actual genome-wide pharmacogenomics study

In this paper, we focus on the elimination rate constant (K_{el}), which is the first order rate constant describing drug elimination from the body, and report the results of PK-related SNPs associated with K_{el}. The histogram for the K_{el} is shown in Figure 2. The PK data seem to be skewed to the left tail of the distribution; therefore we transformed data before applying both maximum contrast methods by taking the natural logarithm of the observed values.

Table 4 summarizes the number of significant SNPs for various P-value cutoffs by each method. For the P-value cutoff of 0.001, 84 SNPs are significant by the Kruskal–Wallis test, 77 SNPs by the maximum contrast method and 84 SNPs by the modified maximum contrast method. Two SNPs (GLT25D1: rs3848643 and BCNP1: rs6512201) are detected as additive model by all three methods in Table 5. In considering a multiple testing problem, we assume the existence of about 10 000 linkage disequilibrium blocks within 100 000 gene-centric SNPs, which are concentrated in about 2% of the human genome (that is, average interval of two SNPs is 600 bp). It follows that the P-value cutoff is set at 5.0×10^{-6} as Bonferroni correlation. As a result, two SNPs (rs2148582, rs699) in angiotensinogen (*AGT*) gene are detected as a dominant model by both the maximum contrast method and modified maximum contrast method, but no SNPs are detected by the Kruskal–Wallis test. We show all of the results for association between PK parameters and SNPs at Genome Medicine Database of Japan (http://gemdbj.nibio.go.jp).

Discussion

We reviewed the current methodology for analyzing PK-SNP data in pharmacogenomics studies. We proposed a modified maximum contrast method for detecting a PK-genotype response pattern under unbalanced sample size. The simulation study suggested that both the maximum contrast method and the modified maximum contrast method were more useful for screening PK-related SNPs in consideration of genetic models than is the Kruskal–Wallis test, and that under unbalanced sample size, the modified maximum contrast method was more powerful for detecting true response patterns than the maximum contrast method in the additive and dominant pattern, whereas the maximum contrast method is more powerful than the modified maximum contrast method in the recessive model.

Table 1 The R_p and R_{TP} for various response patterns

Δ	MAF	True situation		Judgment			
				Additive	Recessive	Dominant	R_P
0			MMCM	0.007	0.017	0.023	0.047
		Additive	MCM	0.007	0.017	0.023	0.047
			K–W	—	—	—	0.049
			MMCM	0.008	0.017	0.017	0.042
	0.50	Recessive	MCM	0.008	0.017	0.017	0.042
			K–W	—	—	—	0.045
			MMCM	0.015	0.024	0.022	0.061
		Dominant	MCM	0.015	0.024	0.023	0.062
			K–W	—	—	—	0.052
			MMCM	0.008	0.002	0.043	0.053
		Additive	MCM	0.009	0.024	0.021	0.054
			K–W	—	—	—	0.051
			MMCM	0.008	0.002	0.043	0.053
	0.25	Recessive	MCM	0.011	0.031	0.019	0.061
			K–W	—	—	—	0.048
			MMCM	0.006	0.000	0.051	0.057
		Dominant	MCM	0.014	0.014	0.023	0.051
			K–W	—	—	—	0.039
			MMCM	0.001	0.000	0.035	0.036
		Additive	MCM	0.004	0.026	0.018	0.048
			K–W	—	—	—	0.050
			MMCM	0.002	0.000	0.042	0.044
	0.12	Recessive	MCM	0.009	0.018	0.017	0.044
			K–W	—	—	—	0.055
			MMCM	0.000	0.000	0.048	0.048
		Dominant	MCM	0.008	0.018	0.025	0.051
			K–W	—	—	—	0.043
0.5			MMCM	0.405	0.140	0.144	0.689
		Additive	MCM	0.408	0.138	0.144	0.690
			K–W	—	—	—	0.628
			MMCM	0.130	0.672	0.005	0.807
	0.50	Recessive	MCM	0.128	0.674	0.005	0.807
			K–W	—	—	—	0.772
			MMCM	0.134	0.012	0.679	0.825
		Dominant	MCM	0.133	0.011	0.682	0.826
			K–W	—	—	—	0.769
			MMCM	0.211	0.041	0.139	0.391
		Additive	MCM	0.135	0.373	0.030	0.538
			K–W	—	—	—	0.452
			MMCM	0.173	0.308	0.009	0.490
	0.25	Recessive	MCM	0.009	0.747	0.001	0.757
			K–W	—	—	—	0.789
			MMCM	0.063	0.000	0.413	0.476
		Dominant	MCM	0.134	0.066	0.238	0.438
			K–W	—	—	—	0.381
			MMCM	0.036	0.002	0.106	0.144
		Additive	MCM	0.043	0.192	0.010	0.245
			K–W	—	—	—	0.267
			MMCM	0.089	0.017	0.027	0.133
	0.12	Recessive	MCM	0.004	0.443	0.001	0.448
			K–W	—	—	—	0.593
			MMCM	0.010	0.000	0.192	0.202
		Dominant	MCM	0.058	0.058	0.072	0.188
			K–W	—	—	—	0.165
1.0			MMCM	0.966	0.019	0.012	0.997
		Additive	MCM	0.968	0.018	0.011	0.997
			K–W	—	—	—	0.998

Table 1 *Continued*

Δ	MAF	True situation		Judgment			
				Additive	*Recessive*	*Dominant*	R_P
			MMCM	0.004	0.996	0.000	1.000
	0.5	Recessive	MCM	0.004	0.996	0.000	1.000
			K–W	—	—	—	1.000
			MMCM	0.002	0.000	0.998	1.000
		Dominant	MCM	0.002	0.000	0.998	1.000
			K–W	—	—	—	1.000
			MMCM	0.764	0.133	0.053	0.950
		Additive	MCM	0.395	0.592	0.001	0.988
			K–W	—	—	—	0.980
			MMCM	0.052	0.944	0.000	0.996
	0.25	Recessive	MCM	0.000	1.000	0.000	1.000
			K–W	—	—	—	1.000
			MMCM	0.042	0.000	0.934	0.976
		Dominant	MCM	0.195	0.041	0.724	0.960
			K–W	—	—	—	0.920
			MMCM	0.390	0.014	0.121	0.525
		Additive	MCM	0.071	0.708	0.003	0.782
			K–W	—	—	—	0.818
			MMCM	0.185	0.485	0.001	0.671
	0.12	Recessive	MCM	0.000	0.964	0.000	0.964
			K–W	—	—	—	0.994
			MMCM	0.033	0.000	0.624	0.657
		Dominant	MCM	0.175	0.151	0.319	0.645
			K–W	—	—	—	0.483

Abbreviations: Δ, given coefficient of response mean value; K–W, Kruskal–Wallis test; MAF, minor allele frequency; MCM, maximum contrast method; MMCM, modified maximum contrast method.
Notation for defining R_P and R_{TP}.
Positive predictive value: $R_{TP} = N_{TP}/N$, power: $R_P = N_R/N$.
Shaded region shows the positive predictive value (R_{TP}) for detection of true response patterns.

In addition, the survey on judgment for PK-related SNPs makes evident that the modified maximum contrast method gave a judgment closer to the judgment of experts than did the maximum contrast method. The expert's judgment was subjective, and also different by each expert. The modified maximum contrast method and the maximum contrast method were able to objectively detect the response pattern and the PK-related SNPs under unbalanced sample size.

The application of the maximum contrast method, modified maximum contrast method and Kruskal–Wallis test to a pharmacogenomics study supported these considerations. When the *P*-value cutoff was set at 0.05 in this application, about 5000 SNPs were detected as statistical significance, and both maximum contrast methods were able to show each genetic model to the biomedical researcher. We showed the list of identified SNPs by each method. The two SNPs in the *AGT* gene showed a statistical significant difference in K_{el} by both the maximum contrast method and modified maximum contrast method, but the Kruskal–Wallis test was not able to detect the gene after multiple testing adjustment. Polymorphic variations in the human *AGT* gene have been shown to be associated with

Table 2 False positive for response patterns

Δ	MAF	Response pattern	K–W	MCM	MMCM
0.5	0.5	Valley I	0.780	0.467	0.455
		Valley II	0.617	0.519	0.513
		Valley III	0.623	0.543	0.540
	0.25	Valley I	0.765	0.304	0.177
		Valley II	0.355	0.259	0.311
		Valley III	0.713	0.493	0.227
	0.12	Valley I	0.515	0.184	0.087
		Valley II	0.213	0.124	0.149
		Valley III	0.546	0.272	0.071
1.0	0.5	Valley I	1.000	0.989	0.987
		Valley II	0.999	0.995	0.995
		Valley III	0.998	0.992	0.991
	0.25	Valley I	1.000	0.937	0.774
		Valley II	0.924	0.746	0.797
		Valley III	1.000	0.988	0.890
	0.12	Valley I	0.991	0.579	0.243
		Valley II	0.687	0.346	0.404
		Valley III	0.996	0.800	0.298

Abbreviations: Δ, given coefficient of response mean value; K–W, Kruskal–Wallis test; MAF, minor allele frequency; MCM, maximum contrast method; MMCM, modified maximum contrast method.

Table 3 Difference in judgment between statistical methods and experts

Modified maximum contrast method		*Maximum contrast method*		*Expert*
P-value	*Judgment*	*P-value*	*Judgment*	*Judgment*
0.007	Additive	<0.00001	Recessive	Additive (5), dominant (1)
0.009	Additive	0.014	Additive	Additive (4), dominant (1), recessive (1)
0.003	Recessive	0.004	Recessive	Recessive (4), additive (1), dominant (1)
0.011	Dominant	0.008	Dominant	Dominant (4), none (2)
<0.00001	Dominant	0.001	Recessive	Dominant (6)
0.998	None	0.999	None	None (6)

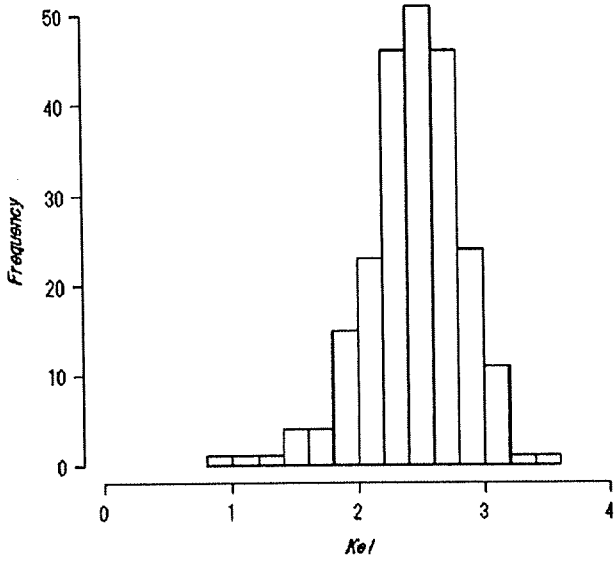

Figure 2 Histogram of elimination rate constant (K_{el}) for the gemcitabine pharmacogenomic (PGx) study.

Table 4 Number of significant SNPs for various *P*-value cutoffs by each method

P-value cutoff	*Method*	*Additive*	*Recessive*	*Dominant*	*Total*
$P \leqslant 0.05$	K–W	—	—	—	4295 SNPs
	MCM	829 SNPs	1768 SNPs	1777 SNPs	4374 SNPs
	MMCM	705 SNPs	239 SNPs	3471 SNPs	4415 SNPs
$P \leqslant 0.01$	K–W	—	—	—	774 SNPs
	MCM	175 SNPs	304 SNPs	385 SNPs	864 SNPs
	MMCM	117 SNPs	51 SNPs	716 SNPs	884 SNPs
$P \leqslant 0.005$	K–W	—	—	—	369 SNPs
	MCM	105 SNPs	146 SNPs	182 SNPs	433 SNPs
	MMCM	59 SNPs	17 SNPs	377 SNPs	453 SNPs
$P \leqslant 0.001$	K–W	—	—	—	84 SNPs
	MCM	16 SNPs	27 SNPs	34 SNPs	77 SNPs
	MMCM	11 SNPs	0 SNPs	73 SNPs	84 SNPs
$P \leqslant 0.0005$	K–W	—	—	—	47 SNPs
	MCM	8 SNPs	15 SNPs	27 SNPs	50 SNPs
	MMCM	6 SNPs	0 SNPs	45 SNPs	51 SNPs
$P \leqslant 0.0001$	K–W	—	—	—	6 SNPs
	MCM	3 SNPs	5 SNPs	9 SNPs	17 SNPs
	MMCM	3 SNPs	0 SNPs	17 SNPs	20 SNPs

Abbreviations: K–W, Kruskal–Wallis test; MCM, maximum contrast method; MMCM, modified maximum contrast method; SNPs, single nucleotide polymorphisms.

increased circulating AGT concentrations,[18] an increased risk of essential hypertension,[18–22] and a decline in renal function.[23] Although it is possible that the *AGT* gene polymorphisms influence gemcitabine PK through yet unknown mechanisms, the result and the suggested hypothesis in our study should be evaluated both in replication study using another sample set and also in biological functional analyses.

Many biomedical researchers have used the Kruskal–Wallis test for finding significant SNPs, and visually checked PK-genotype response patterns. Recently, powerful array-based SNP typing platforms have heralded an era in which a genome-wide association study is a popular or standard strategy for identifying disease associated genes or drug response genes for common diseases, and genotype data on 100 000–1 000 000 SNPs are increasingly available to researchers. It is virtually impossible for biomedical researchers to visually check the response patterns on such a genome scan data. Our 'study has proposed an alternative by showing that either a modified maximum contrast method or a maximum contrast method can readily be applied to genome scans as a statistical screening method.

Materials and methods

Maximum contrast method and modified maximum contrast method

We first describe a general form for a maximum contrast method as discussed in Yoshimura *et al.*,[14] and Wakana *et al.*,[17] in a pharmacogenomics study. We assume Y_{ij} ($i = 1, 2, 3$; $j = 1, 2, \ldots, n_i$) as an observed response for jth individual in ith genotype group (*AA*, *Aa* and *aa*, where '*A*' is major

Table 5 List of identified SNPs by each method

Gene information				K–W	MCM		MMCM	
Chr	*RS #*	*Allele*	*Gene*	*P-value*	*P-value*	*Pattern*	*P-value*	*Pattern*
1	rs2148582	A/G	*AGT*	0.011	1.5×10^{-9}	Dominant	8.6×10^{-7}	Dominant
1	rs699	C/T	*AGT*	0.012	1.5×10^{-9}	Dominant	1.4×10^{-6}	Dominant
3	rs1132979	C/G	*eIF2A*	4.1×10^{-4}	2.7×10^{-4}	Additive	1.0×10^{-4}	Dominant
4	rs11736926	C/G	*NDST4*	0.0046	3.4×10^{-4}	Dominant	1.0×10^{-4}	Dominant
6	rs1932523	A/G	*FILIP1*	0.0073	2.7×10^{-4}	Dominant	1.0×10^{-4}	Dominant
6	rs2223869	C/T	*TFAP2B*	8.8×10^{-5}	0.25	Recessive	0.48	Recessive
6	rs2703702	A/G	*FILIP1*	0.0027	1.0×10^{-4}	Dominant	1.0×10^{-4}	Dominant
7	rs12667496	C/T	*HIC*	0.0070	8.9×10^{-6}	Recessive	0.0015	Dominant
8	rs2938303	A/G	*OXR1*	4.2×10^{-4}	1.0×10^{-4}	Additive	1.0×10^{-4}	Additive
9	rs4149336	C/T	*ABCA1*	0.0049	3.3×10^{-4}	Dominant	2.8×10^{-4}	Dominant
9	rs4842151	C/T	*COL5A1*	2.7×10^{-5}	5.2×10^{-5}	Recessive	0.0032	Additive
9	rs4842152	C/T	*COL5A1*	8.4×10^{-5}	7.6×10^{-5}	Recessive	0.0023	Additive
12	rs4763797	A/G	*LRP6*	0.033	2.4×10^{-5}	Dominant	1.0×10^{-4}	Dominant
14	rs1243459	C/T	*C14orf8*	0.003	1.7×10^{-4}	Dominant	1.0×10^{-4}	Dominant
15	rs2271714	A/G	*MFGE8*	0.002	1.0×10^{-4}	Dominant	1.0×10^{-4}	Dominant
17	rs2233362	A/G	*GNGT2*	3.5×10^{-4}	2.0×10^{-4}	Dominant	1.0×10^{-4}	Dominant
18	rs12607882	C/T	*METTL4*	5.0×10^{-5}	0.057	Recessive	0.28	Recessive
19	rs3848643	C/T	*GLT25D1*	6.8×10^{-5}	8.1×10^{-5}	Additive	6.2×10^{-5}	Additive
19	rs6512201	C/G	*BCNP1*	5.2×10^{-5}	5.3×10^{-5}	Additive	4.3×10^{-5}	Additive
21	rs9647237	C/T	*C21orf12*	0.042	2.0×10^{-8}	Dominant	4.4×10^{-5}	Dominant
22	rs1008530	C/T	*TFIP11*	0.0018	2.0×10^{-4}	Dominant	1.0×10^{-4}	Dominant
22	rs1894704	A/C	*HPS4*	4.9×10^{-4}	1.8×10^{-5}	Dominant	1.0×10^{-4}	Dominant
22	rs1894705	C/T	*HPS4*	5.7×10^{-4}	1.3×10^{-5}	Recessive	3.1×10^{-4}	Dominant
22	rs3752589	G/T	*HPS4*	5.7×10^{-4}	1.4×10^{-5}	Recessive	3.1×10^{-4}	Dominant
22	rs5761557	A/G	*HPS4*	5.7×10^{-4}	1.1×10^{-5}	Recessive	1.0×10^{-4}	Dominant
22	rs713998	A/G	*HPS4*	4.9×10^{-4}	2.2×10^{-5}	Dominant	1.1×10^{-5}	Dominant
22	rs737800	C/T	*HPS4*	3.9×10^{-4}	3.4×10^{-5}	Dominant	1.0×10^{-4}	Dominant

Abbreviations: Chr, chromosome number; K–W, Kruskal–Wallis test; MCM, maximum contrast method; MMCM, modified maximum contrast method; RS#, dbSNP reference SNP identification number.
Shaded region is the identified SNPs by each method (*P*-value$\leqslant$0.0001).

allele, and '*a*' is minor allele), and Y_{ij}s are independently and normally distributed with $E(Y_{ij}) = \mu_i$ and $\mathrm{Var}(Y_{ij}) = \sigma^2$. Under these conditions, $\bar{\boldsymbol{Y}} = (\bar{Y}_1, \bar{Y}_2, \bar{Y}_3)^t$ follows the trivariate normal distribution $N(\mu, \sigma^2 D)$ where

$$\bar{Y}_i = \frac{1}{n_i}\sum_{j=1}^{n_i} Y_{ij},\ \boldsymbol{\mu} = (\mu_1, \mu_2, \mu_3)^t \quad \text{and}$$

$$\boldsymbol{D} = \mathrm{diag}\left(\frac{1}{n_1}, \frac{1}{n_2}, \frac{1}{n_3}\right),$$

diag(●) being a diagonal matrix, and the superscript t indicates the transpose of a matrix or vector. In the maximum contrast method, some contrast statistics are set according to the approach. Let contrast statistic T_k with a coefficient $\boldsymbol{c_k} = (c_{k1}, c_{k2}, c_{k3})^t$ where $c_{k1} + c_{k2} + c_{k3} = 0$, and $k = 1$, 2 and 3 correspond to an additive, recessive and dominant response pattern, respectively, as shown in Figure 1. The following coefficients were used for each genetic model:

$$\begin{aligned} c_1 &= (-1 \quad 0 \quad 1)^t, \\ c_2 &= (-2 \quad 1 \quad 1)^t, \\ c_3 &= (-1 \quad -1 \quad 2)^t. \end{aligned}$$

The contrast statistics is defined in terms of the contrast vector c_k,

$$T_k = \frac{c_k^t \bar{Y}}{\sqrt{\hat{\sigma}^2 c_k^t D c_k}}, \tag{1}$$

where $\hat{\sigma}^2$ is $\frac{1}{\gamma}\sum_{i=1}^{3}\sum_{j=1}^{n_i}(y_{ij} - \bar{y}_i)^2$, and $\gamma = \sum_{i=1}^{3} n_i - 3$ is degree of freedom of $\hat{\sigma}^2$. Then the statistic is defined as:

$$T_{\max} = \max(T_1, T_2, T_3). \tag{2}$$

The statistics can be used to test over null hypotheses, H_0: $\mu_1 = \mu_2 = \mu_3$, on the other hand, in pharmacogenomics studies, alternative hypotheses such as H_1: $\mu_1 < \mu_2 < \mu_3$, $\mu_1 = \mu_2 < \mu_3$, $\mu_1 < \mu_2 = \mu_3$. The *P*-value for the probability distribution of $T_{\max}$ under the over null hypotheses is calculated by using the complex property of integration in the multivariate *t*-distribution with singular correlation matrix,[24] and the *P*-value is defined as in the following formula:

$$\begin{aligned} P\text{-value} &= \Pr(t_{\max} > t^*_{\max} | H_0) = 1 - \Pr(t_{\max} \geqslant t^*_{\max}) \\ &= 1 - \Pr(t_1 < t^*_{\max},\ t_2 < t^*_{\max},\ t_3 < t^*_{\max}) \end{aligned}, \tag{3}$$

where $t^*_{\max}$ is the observed value of the test statistics.

This method can select the response pattern, which best fits the observed data among a set of patterns. In clinical and

toxicological trials, the sample size of each group is almost equivalent; therefore the maximum contrast method assumes an equivalent sample size of each group. However, the sample size of each group is not equivalent in pharmacogenomics studies, because the MAF is less than 0.5 and is generally around 0.2. For this reason, under the unbalanced sample size, the adjoining denominator of contrast statistic $\sqrt{\left(\frac{c_{k1}^2}{n_1}+\frac{c_{k2}^2}{n_2}+\frac{c_{k3}^2}{n_3}\right)\hat{\sigma}^2}$ is overestimated although the studentized statistics by this variance estimate is robust. Therefore, the maximum contrast method cannot be applied for detecting a true response pattern in pharmacogenomics studies.

Here we propose a modified maximum contrast method for unbalanced sample size. First, the modified contrast statistic is given by

$$T'_k = \frac{\boldsymbol{c}_k^t \bar{\boldsymbol{Y}}}{\sqrt{\boldsymbol{c}_k^t \boldsymbol{c}_k}}, \tag{4}$$

thus the adjoining denominator of the modified contrast statistic is $\sqrt{c_{k1}^2 + c_{k2}^2 + c_{k3}^2}$, and it is not influenced by unbalanced sample size. The modified maximum contrast statistic is given by

$$T'_{\max} = \max(T'_1, T'_2, T'_3). \tag{5}$$

In addition, the multiplicity adjusted *P*-value for the probability distribution of $T'_{\max}$ under H_0 was calculated by the permutation procedure.[25] Simple random sampling without replacement method generates the sampling distribution of the statistic by drawing repeated samples from the observed sample itself. Consequently, the permutation procedure is used to simulate *P*-values; the lowest *P*-value is calculated for each of 100 000 permutations for the entire dataset, and from this distribution.

Simulation study

We assess the power of the Kruskal–Wallis test, the maximum contrast method (Equations (1) and (2)) and the modified maximum contrast method (Equations (4) and (5)) by simulation studies. The scenarios discussed here are motivated by the anticancer drug's pharmacogenomics data that will be introduced below. In particular, we are interested in the performance of all three tests when the MAF decreases. To examine these effects, we simulate PK parameter data from transformed log-normal distribution by each genotype. The distributions of PK parameters are often unknown, but empirically are modeled under the assumption of a log-normal distribution because (1) PK parameter values must be nonnegative and the normal assumption does not enforce this assumption; (2) distribution of estimated PK parameters is often left skewed, which is compatible with a log-normal distribution.[26] Here, for applying an intravenous anticancer drug in actual data, we focus on the elimination rate constant (K_{el}), which is the first order rate constant describing drug elimination from the body. We assume that a sample of patients with any genotype (*AA*, *Aa* or *aa*) and the proportion of MAF is given, and that this population is in HWE. For each patient, the PK parameter, K_{el} is given. Under these assumptions, we generated K_{el} by each genotype from the log-normal distribution with mean μ_i, that is, $\bar{Y}_i \sim \mathrm{LN}(\mu_i, 1)$, $i = 1, 2, 3$ in *i*th genotype group (*AA*, *Aa* and *aa*), where $\mu_i = \Delta \cdot c_{ki}$ and Δ is given coefficient and c_{ki} corresponded to element of contrast statistics vector $\boldsymbol{c}_k = (c_{k1}\ c_{k2}\ c_{k3})^t$. Here, Δ is set at 0.0, 0.5 and 1.0, respectively, and the contrast statistics vectors are set as the following coefficients corresponding to the genetic models ($k = 1$, 2 and 3) in Figure 1 (i)–(iii):

$$\boldsymbol{c}_1 = (-1\ \ 0\ \ 1)^t,$$
$$\boldsymbol{c}_2 = (-2\ \ 1\ \ 1)^t,$$
$$\boldsymbol{c}_3 = (-1\ \ -1\ \ 2)^t.$$

In addition, the MAF was set at 0.12, 0.25 or 0.50, respectively, where total sample size (n) was 300 or 600 subjects. The criteria to evaluate the performance of each method were two indicators, R_P and R_{TP}, defined by Equations (6) and (7).

$$R_P = \frac{N_R}{N}, \tag{6}$$

$$R_{TP} = \frac{N_{TP}}{N}. \tag{7}$$

R_p is a proportion of detected PK-related SNPs (power), whereas R_{TP} is the proportion of detected true response patterns among PK-related SNPs (positive predictive value). The Monte-Carlo simulation to calculate R_p and R_{TP} was repeated 10 000 times and the mean values of indicators were calculated. Note that N was a constant fixed as the repetition number of the simulation, whereas N_R was a random variable realized as the number of rejections by the hypothesis test, and N_{TP} was the number of detected true response patterns.

Questionnaire survey on judgment

To identify PK-related genes, biological experts who are pharmacokinetists, molecular biologists and geneticists used to draw box-and-whisker plots on PK parameters by each genotype, and check these response patterns by sight. This judgment involves much experience, but it is subjective and may differ by expert. We conducted a questionnaire survey to compare statistical judgment with judgment by experts. First, we showed summary statistics and box–whisker plot (Figure 3) to the expert group that consisted of two pharmacokinetists, two molecular biologists and two geneticists. Second, these experts independently gave a decision from six response patterns (Figure 1). Finally, we applied the modified maximum contrast method and the maximum contrast method to this survey dataset, and, by using Kendall's rank correlation coefficient, evaluated, which method is closer to expert judgment.

Application to actual gemcitabine pharmacogenomics study

We applied the Kruskal–Wallis test, the maximum contrast method and the modified maximum contrast method to an actual genome-wide pharmacogenomics study on antitumor drugs. The study was performed within the Millennium Genome Project in Japan, and four antitumor drugs were

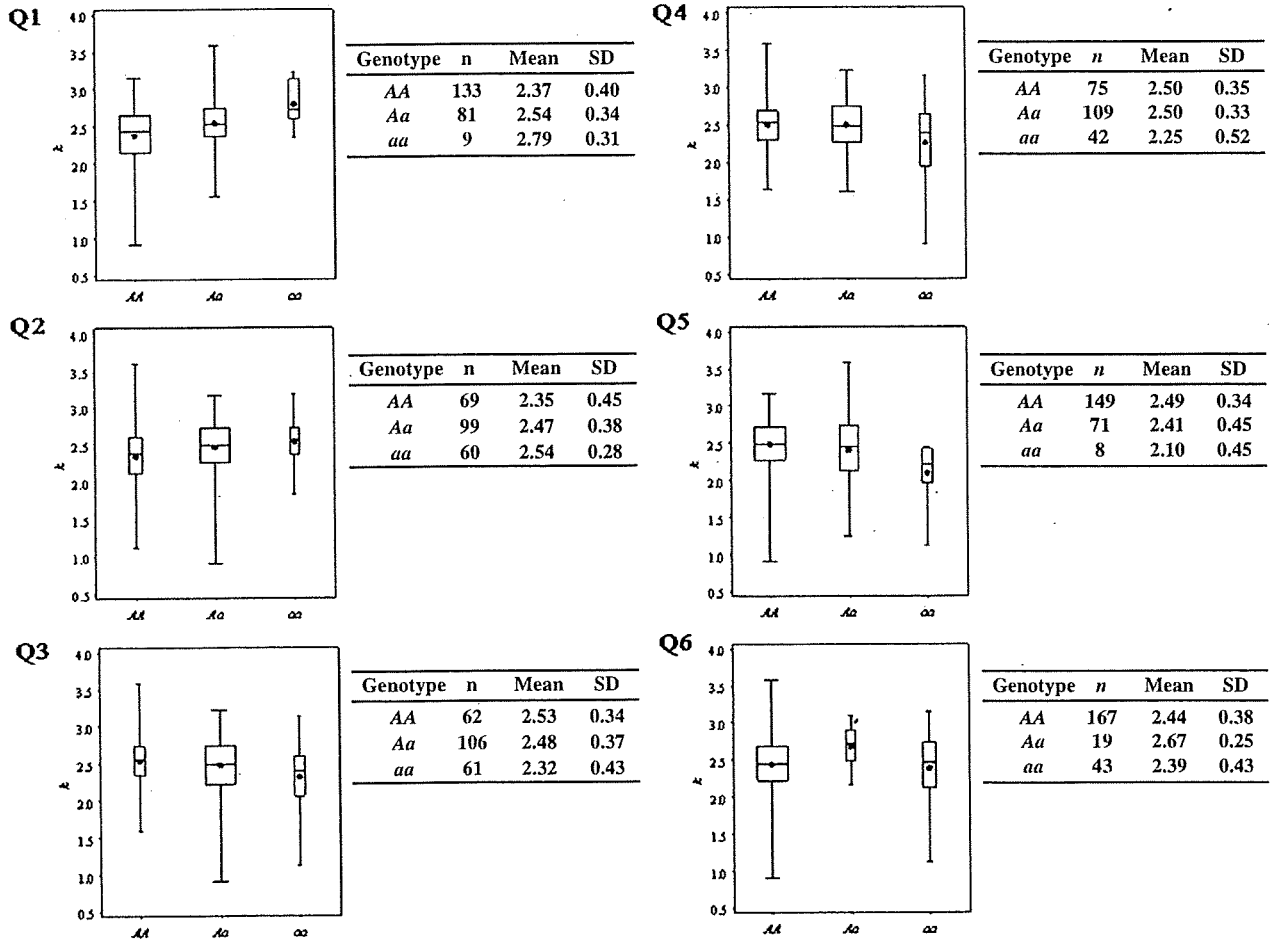

Figure 3 Summary statistics and box–whisker plot in questionnaire survey.

chosen as project targets: irinotecan, fluorouracil, paclitaxel and gemcitabine. One or some combination of the drugs was administered to about 1000 cancer patients with written informed consent at the National Cancer Center, Japan. PK data were also obtained for the drugs except for fluorouracil. In addition, about 1000 DNA samples were extracted from peripheral blood mononuclear cells and 109 365 SNPs were genotyped by Illumina Human-1 BeadChip.

In this application, we emphasize a focus on the gemcitabine pharmacogenomics study. Gemcitabine (2′,2′-difluorodeoxycytidine) is a nucleoside anticancer drug that has a broad spectrum of antitumor activity against various solid tumors, such as nonsmall cell lung cancer and pancreatic cancer. The participants consisted of 256 Japanese gemcitabine-naive cancer patients (mainly pancreatic carcinoma) at the National Cancer Center Hospital and National Cancer Center Hospital East. Details of this analysis group were reported previously.[27] For gemcitabine PK analysis, 5 ml of heparinized blood was sampled before the first gemcitabine administration, and at 0, 15, 30, 60, 90, 120 and 240 min after the termination of the infusion. The AUC, mean residence time from 0 to infinity, peak concentration (C_{max}), clearance (CL m^{-2}), distribution volume based on the terminal phase (Vz m^{-2}) and elimination rate constant (K_{el}) were calculated using WinNonlin ver. 4.01 (Pharsight Corporation, Mountain View, CA, USA). For an investigation of the association between these PK parameters and SNPs in Illumina Human-1 BeadChip, we applied the maximum contrast method, the modified maximum contrast method and the Kruskal–Wallis test.

Acknowledgments

We thank Professor Isao Yoshimura and Professor Chikuma Hamada at Tokyo University of Science for their valuable advice, and Dr Hiromi Sakamoto and Ms Sumiko Ohnami for the SNP genotyping. Yasunori Sato is a recipient of Official Trainee of the Foreign Clinical Pharmacology Training Program, Japanese Society of Clinical Pharmacology and Therapeutics. This work was initiated while Yasunori Sato was a postdoctoral fellow at the Department of Biostatistics, Harvard School of Public Health, and partially supported in Japan by the program for promotion of Fundamental Studies in Health Sciences of the National Institute of Biomedical Innovation (NiBio).

Duality of interest

None declared.

References

1 Licinio J, Wong M. *Pharmacogenomics: The Search for Individualized Therapies*. Wiley: Weinheim (Germany), 2002.
2 Evans WE, McLeod HL. Pharmacogenomics—drug disposition, drug targets, and side effects. *N Engl J Med* 2003; **348**: 538–549.
3 Ingelman-Sundberg M. Pharmacogenomic biomarkers for prediction of severe adverse drug reactions. *N Engl J Med* 2008; **358**: 637–639.
4 Efferth T, Volm M. Pharmacogenetics for individualized cancer chemotherapy. *Pharmacol Ther* 2005; **107**: 155–176.
5 US FDA. Guidance for Industry Pharmacogenomic Data Submissions. 2005.
6 International Human Genome Sequencing Consortium. Finishing the euchromatic sequence of the human genome. *Nature* 2004; **431**: 931–945.
7 Risch N, Merikangas K. The future of genetic studies of complex human diseases. *Science* 1996; **273**: 1516–1517.
8 Hirschhorn JN, Daly MJ. Genome-wide association studies for common diseases and complex traits. *Nat Rev Genet* 2005; **6**: 95–108.
9 Kingsmore SF, Lindquist IE, Mudge J, Gessler DD, Beavis WD. Genome-wide association studies: progress and potential for drug discovery and development. *Nat Rev Drug Discov* 2008; **7**: 221–230.
10 Kruskal HW, Wallis WA. Use of ranks in one-criterion variance analysis. *J Am Stat Assoc* 1952; **47**: 583–621.
11 Siegel S, Castellan NJ. *Nonparametric Statistics for the Behavioral Sciences*, 2nd edn. McGraw-Hill: New York, 1988.
12 Mukerjee H, Robertson T, Wright FT. Comparison of several treatments with a control using multiple contrast. *J Am Stat Assoc* 1987; **82**: 902–910.
13 Ruberg SJ. Contrasts identifying the minimum effective dose. *J Am Stat Assoc* 1989; **82**: 816–822.
14 Yoshimura I, Wakana A, Hamada C. A performance comparison of maximum contrast methods to detect dose dependency. *Drug Inf J* 1997; **31**: 423–432.
15 Stewart H, Ruberg SJ. Detecting dose response with contrasts. *Stat Med* 2000; **19**: 913–921.
16 Nishiyama H, Yanagihara H, Yoshimura I. SAS/IML program for computing probabilities related to maximum contrast methods. *Jpn J Biometrics* 2003; **24**: 57–70, (in Japanese).
17 Wakana A, Yoshimura I, Hamada C. A method for therapeutic dose selection in a phase II clinical trial using contrast statistics. *Stat Med* 2007; **26**: 498–511.
18 Jeunemaitre X, Soubrier F, Kotelevtsev YV, Lifton RP, Williams CS, Charru A *et al.* Molecular basis of human hypertension: role of angiotensinogen. *Cell* 1992; **71**: 169–180.
19 Caulfield M, Lavender P, Farrall M, Munroe P, Lawson M, Turner P *et al.* Linkage of the angiotensinogen gene to essential hypertension. *N Engl J Med* 1994; **330**: 1629–1633.
20 Hegele RA, Brunt JH, Connelly PW. A polymorphism of the angiotensinogen gene associated with variation in blood pressure in a genetic isolate. *Circulation* 1994; **90**: 2207–2212.
21 Vasku A, Soucek M, Znojil V, Rihacek I, Tschoplova S, Strelcova L *et al.* Angiotensin I-converting enzyme and angiotensinogen gene interaction and prediction of essential hypertension. *Kidney Int* 1998; **53**: 1479–1482.
22 Pereira TV, Nunes AC, Rudnicki M, Yamada Y, Pereira AC, Krieger JE. Meta-analysis of the association of 4 angiotensinogen polymorphisms with essential hypertension: a role beyond M235T? *Hypertension* 2008; **51**: 778–783.
23 Pei Y, Scholey J, Thai K, Suzuki M, Cattran D. Association of angiotensinogen gene T235 variant with progression of immunoglobulin A nephropathy in Caucasian patients. *J Clin Invest* 1997; **100**: 814–820.
24 Genz A, Bretz F. Numerical computation of multivariate t-probabilities with application to power calculation of multiple contrasts. *J Stat Comput Simulat* 1999; **63**: 361–378.
25 Westfall PH, Young SS. *Resampling-Based Multiple Testing: Examples and Methods for P-value Adjustment*. Wiley: New York, 1993.
26 Gabrielsson J, Weiner D. *Pharmacokinetic and Pharmacodynamic Data Analysis: Concepts and Applications*. Taylor & Francis: Sweden, 2000.
27 Sugiyama E, Kaniwa N, Kim SR, Kikura-Hanajiri R, Hasegawa R, Maekawa K *et al.* Pharmacokinetics of gemcitabine in Japanese cancer patients: the impact of a cytidine deaminase polymorphism. *J Clin Oncol* 2007; **25**: 32–42.

VOLUME 27 · NUMBER 13 · MAY 1 2009

JOURNAL OF CLINICAL ONCOLOGY

ORIGINAL REPORT

Identification of a Predictive Biomarker for Hematologic Toxicities of Gemcitabine

Junichi Matsubara, Masaya Ono, Ayako Negishi, Hideki Ueno, Takuji Okusaka, Junji Furuse, Koh Furuta, Emiko Sugiyama, Yoshiro Saito, Nahoko Kaniwa, Junichi Sawada, Kazufumi Honda, Tomohiro Sakuma, Tsutomu Chiba, Nagahiro Saijo, Setsuo Hirohashi, and Tesshi Yamada

From the Chemotherapy Division, National Cancer Center Research Institute; Hepatobiliary and Pancreatic Oncology Division and Clinical Laboratory Division, National Cancer Center Hospital; Project Team for Pharmacogenetics, National Institute of Health Sciences; BioBusiness Group, Mitsui Knowledge Industry, Tokyo; Hepatobiliary and Pancreatic Oncology Division, National Cancer Center Hospital East, Kashiwa; and Department of Gastroenterology and Hepatology, Kyoto University Graduate School of Medicine, Kyoto, Japan.

Submitted September 3, 2008; accepted December 1, 2008; published online ahead of print at www.jco.org on March 16, 2009.

Supported by the Program for Promotion of Fundamental Studies in Health Sciences conducted by the National Institute of Biomedical Innovation of Japan, the Third-Term Comprehensive Control Research for Cancer conducted by the Ministry of Health and Labor of Japan, and generous grants from the Naito Foundation, the Princess Takamatsu Cancer Research Fund, and the Foundation for the Promotion of Cancer Research. These sponsors had no role in the design of the study, the collection of the data, the analysis and interpretation of the data, the decision to submit the article for publication, or the writing of the article

Authors' disclosures of potential conflicts of interest and author contributions are found at the end of this article.

Corresponding author: Tesshi Yamada, MD, PhD, Chemotherapy Division, National Cancer Center Research Institute, 5-1-1 Tsukiji, Chuo-ku, Tokyo 104-0045, Japan; e-mail: tyamada@ncc.go.jp.

The Appendix is included in the full-text version of this article, available online at www.jco.org. It is not included in the PDF version (via Adobe® Reader®).

0732-183X/09/2713-2261/$20.00

DOI: 10.1200/JCO.2008.19.9745

ABSTRACT

Purpose
Gemcitabine monotherapy is the current standard for patients with advanced pancreatic cancer, but the occurrence of severe neutropenia and thrombocytopenia can sometimes be life threatening. This study aimed to discover a new diagnostic method for predicting the hematologic toxicities of gemcitabine.

Patients and Methods
Using quantitative mass spectrometry (MS), we compared the baseline plasma proteomes of 25 patients who had developed severe hematologic adverse events (grade 3 to 4 neutropenia and/or grade 2 to 4 thrombocytopenia) within the first two cycles of gemcitabine with those of 22 patients who had not (grade 0).

Results
We identified 757 peptide peaks whose intensities were significantly different ($P < .001$, Welch t test) among a total of 60,888. The MS peak with the highest statistical significance ($P = .0000282$) was revealed to be derived from haptoglobin by tandem MS. A scoring system (nomogram) based on the values of haptoglobin, haptoglobin phenotype, neutrophil count, platelet count, and body-surface area was constructed to estimate the risk of hematologic adverse events (grade 3 to 4 neutropenia and/or grade 2 to 4 thrombocytopenia) with an area under curve value of 0.782 in a cohort of 166 patients with pancreatic cancer. Predictive ability of the system was confirmed in two independent validation cohorts consisting of 87 and 52 patients with area under the curve values of 0.655 and 0.747, respectively.

Conclusion
Although the precise mechanism responsible for the correlation of haptoglobin with the future onset of hematologic toxicities remains to be clarified, our prediction model seems to have high practical utility for tailoring the treatment of patients receiving gemcitabine.

J Clin Oncol 27:2261-2268. © 2009 by American Society of Clinical Oncology

INTRODUCTION

Pancreatic adenocarcinoma is one of the most aggressive and lethal cancers.[1] It is the fifth leading cause of cancer-related mortality in Japan and the fourth leading cause in the United States, accounting for an estimated more than 23,000 annual deaths in Japan and more than 33,000 deaths in the United States.[2,3] The median survival time of patients with advanced pancreatic cancer had remained at only 3 to 4 months until the introduction of the nucleoside anticancer drug gemcitabine (2′,2′-difluorodeoxycytidine). Gemcitabine monotherapy extended the overall survival of pancreatic cancer patients up to 6 months, along with significant clinical benefits such as pain relief and improvement of performance status,[4-6] and is now accepted as a standard first-line treatment for unresectable advanced pancreatic cancer.[7] However, hematologic toxicity is the dose-limiting factor of gemcitabine therapy.[8] Although severe nonhematologic toxicity is infrequent,[4-6] 20% to 30% of patients receiving gemcitabine experience grade 3 to 4 neutropenia (National Cancer Institute [NCI] Common Toxicity Criteria, version 2.0), and approximately 10% experience grade 3 to 4 thrombocytopenia.[5,6,9,10] These levels of severe hematologic adverse events (AEs) can be potentially life threatening.

Several attempts have been made to predict the occurrence of AE associated with chemotherapy. Old age, poor performance status, and reduced initial blood cell counts have been reported to be the risk factors of hematotoxicities.[11,12] To further improve prediction accuracy, combinations of these

risk factors have also been proposed,[11-14] but no reliable predictor has been established for gemcitabine-induced hematologic AEs. We previously identified a significant correlation of a nonsynonymous single nucleotide polymorphism of the cytidine deaminase (*CDA*) gene with altered pharmacokinetics of gemcitabine, but its prediction accuracy for hematologic AE was not satisfactory.[15,16]

Recent advanced proteomic technologies have been increasingly applied to studies of clinical samples[17] to identify biomarkers that could facilitate the tailoring of cancer treatments. Protein expression is not always correlated with mRNA expression,[18] and it is anticipated that alterations in the protein content of clinical samples more directly reflect the biologic and pathologic status of patients. Matrix-assisted laser desorption/ionization mass spectrometry (MS) is becoming a method of choice for profiling of clinical samples as a result of its high sensitivity and throughput. In fact, previous studies have successfully identified biomarkers that could predict the outcome of cancer patients and the efficacy of molecular-targeting drugs.[19,20] However, only low molecular weight proteins can be analyzed by matrix-assisted laser desorption/ionization MS, and thus, a method allowing more comprehensive protein profiling is desirable.

Shotgun proteomics is an emerging concept in which whole proteins are enzymatically digested into a large array of small peptide fragments having uniform physical and chemical characteristics and then analyzed directly by MS. We previously developed a new platform, namely two-dimensional image converted analysis of liquid chromatography and mass spectrometry (2DICAL), to give a quantitative dimension to shotgun proteomics.[21] To identify new biomarkers that might be useful for prediction of gemcitabine-induced neutropenia and thrombocytopenia in patients with pancreatic cancer, we compared the plasma protein profiles of two extreme populations of patients who had shown different responses to the same gemcitabine treatment by 2DICAL. Here we report the identification of plasma/serum haptoglobin as a biomarker of hematologic toxicities associated with gemcitabine treatment.

PATIENTS AND METHODS

Patients

Plasma or serum samples were collected from three cohorts (modeling [M0], validation-1 [V1], and validation-2 [V2] cohorts) totaling 305 patients. All the patients had locally advanced or metastatic (stage IVA or IVB),[22] histologically or cytologically proven pancreatic ductal adenocarcinoma and received at least two cycles of gemcitabine monotherapy (1,000 mg/m^2 intravenously over 30 minutes on days 1, 8, and 15 of a 28-day cycle). Demographic and laboratory data for the patients before administration of gemcitabine are listed in Appendix Tables A1 to A3 (online only). The severity of early hematologic AEs that appeared within the first two cycles of the gemcitabine treatment was graded according to NCI Common Terminology Criteria for Adverse Events (CTCAE; version 3.0).

Cohort M0 comprised 166 patients who had been enrolled onto our previous study at the National Cancer Center (NCC) Hospital (Tokyo, Japan) and Hospital East (Kashiwa, Japan) between September 2002 and July 2004.[15,16] Cohort V1 comprised 87 patients who had been treated consecutively at the NCC Hospital between August 2005 and June 2007, and cohort V2 comprised 52 patients treated at the NCC Hospital consecutively between August 2004 and July 2005.

Sample Preparation

Blood was drawn before the administration of gemcitabine. Plasma (cohorts M0 and V1) or serum (cohort V2) was separated by centrifugation at 4°C and frozen at −70°C (cohort M0) or −20°C (cohorts V1 and V2) until analysis. Macroscopically hemolyzed samples were excluded from the current analysis. The protocol of this retrospective study was reviewed and approved by the institutional ethics committee boards of the NCC (Tokyo, Japan) and the National Institute of Health Sciences (Tokyo, Japan).

Liquid Chromatography/MS

Samples were passed through an IgY-12 High Capacity Spin Column (Beckman Coulter, Fullerton, CA) in accordance with the manufacturer's instructions to reduce the amounts of the 12 most abundant plasma proteins. The flow-through portion was digested with sequencing-grade modified trypsin (Promega, Madison, WI) and analyzed in triplicate using a nano-flow high-performance liquid chromatograph (NanoFrontier nLC; Hitachi High-Technologies, Tokyo, Japan) connected to an electrospray ionization quadrupole time-of-flight (ESI-Q-TOF) mass spectrometer (Q-Tof Ultima; Waters, Milford, MC).

MS peaks were detected, normalized, and quantified using the in-house 2DICAL software package, as described previously.[21] A serial identification (ID) number was applied to each of the MS peaks detected (1 to 60,888). The stability of liquid chromatography/MS was monitored by calculating the correlation coefficient of every triplicate measurement. The mean correlation coefficient (± standard deviation) of the entire 60,888 peaks of the 47 triplicate runs was as high as 0.978 (±0.017).

Tandem MS

Peak lists were generated using the Mass Navigator software package (version 1.2; Mitsui Knowledge Industry, Tokyo, Japan) and searched against the SwissProt database (downloaded from http://www.expasy.ch/sprot/sprot-top.html on October 18, 2007) using the Mascot software package (version 2.2.1; Matrix Science, London, United Kingdom). The score threshold was set to $P < .05$ based on the size of the database used in the search.

Western Blot Analysis

Primary antibodies used were rabbit polyclonal antibody against human haptoglobin (Dako, Glostrup, Denmark) and mouse monoclonal antibody against human complement C3b-α (Progen, Heidelberg, Germany). Ten microliters of partitioned sample were separated by sodium dodecyl sulfate–polyacrylamide gel electrophoresis (SDS-PAGE) and electroblotted onto a polyvinylidene difluoride membrane. The membrane was then incubated with the primary antibody and subsequently with relevant horseradish peroxidase–conjugated antirabbit or antimouse immunoglobulin G as described previously.[23,24] Blots were developed using an enhanced chemiluminescence (ECL) detection system (GE Healthcare, Buckinghamshire, United Kingdom).

Quantification and Subtyping of Haptoglobin

The concentration of plasma or serum haptoglobin was measured using an automated immunonephelometry BN-II system (Siemens Healthcare Diagnostics, Tokyo, Japan). The phenotype of haptoglobin α-chain was determined by nondenaturing (native) SDS-PAGE.[25]

Categorization of Hematologic Toxicities

Overall severity of hematologic toxicities after gemcitabine treatment was classified into categories I to IV based on the worst CTCAE grades of neutropenia and thrombocytopenia (Appendix Fig A1, online only), as follows: category I, grade 0 to 1 neutropenia and grade 0 thrombocytopenia; category II, grade 2 neutropenia or grade 1 thrombocytopenia; category III, grade 3 neutropenia or grade 2 thrombocytopenia; and category IV, grade 4 neutropenia or grade 3 to 4 thrombocytopenia.

Statistical Analysis

Statistical significance of intergroup differences was assessed using the Welch t test, χ^2 test, Wilcoxon test, or Kruskal-Wallis test, as appropriate. Multivariate regression analysis was performed using ordinal logistic regression modeling. Factors included in the prediction model were selected with a forward stepwise selection procedure using Akaike's Information Criterion (AIC). To correct biased sample sizes of categories, each observation was weighted according to the sample size of its category in the fitting process. The significance of differences between models with and without haptoglobin was assessed with the likelihood ratio test. Statistical analyses were performed using

an open-source statistical language R (version 2.7.0; http://www.r-project.org/) with the optional module design package.

RESULTS

Plasma Proteins Associated With Hematologic AEs

To identify a biomarker that can predict the occurrence of hematologic AEs associated with gemcitabine treatment, we compared the baseline plasma proteome between 25 patients who developed severe AEs (grade 3 to 4 neutropenia and/or grade 2 to 4 thrombocytopenia) and 22 patients who did not (grade 0) using 2DICAL. These levels of hematologic AEs have been used as criteria for dose reduction or postponement of gemcitabine-based treatments.[26-28] There was no significant difference in age, sex, Eastern Cooperative Oncology Group performance status, routine biochemical laboratory data, or pharmacokinetics of gemcitabine[15] (Table 1 and data not shown) between the two extreme groups of patients who were selected from cohort M0, but the patients who experienced severe AEs had significantly lower baseline peripheral-blood leukocyte, neutrophil, and platelet counts than patients without AEs (Table 1).

Among a total of 60,888 independent MS peaks detected within the range of 250 to 1,600 m/z and within the time range 20 to 70 minutes, we found that the mean intensity of triplicates differed significantly in 757 peaks ($P < .001$, Welch t test). Figure 1A is a representative two-dimensional view of all the MS peaks displayed with m/z along the x-axis and the retention time of LC along the y-axis. The 757 MS peaks whose expression differed significantly between patients with severe AEs and patients without AEs are highlighted in red.

One hundred fifteen MS/MS spectra acquired from 200 peaks with the smallest P values were matched to 41 proteins in the database (Mascot score of > 15; Appendix Tables A4 and A5, online only). Notably, MS peaks including one that was decreased in patients with severe AEs with the highest statistical significance ($P = .0000282$; Fig 1B) most recurrently (six times) matched the amino acid sequences of the haptoglobin (*HP*) gene product (Appendix Fig A2, online only). Figure 2A shows the distribution of two representative haptoglobin-derived MS peaks (ID 2062 [at 491 m/z and 44.5 minutes] and ID 5681 [at 602 m/z and 47 minutes]) in patients with severe AEs and without AEs. The differential expression and identification of haptoglobin were confirmed by denaturing SDS-PAGE and immunoblotting (Fig 2B).

Correlation of Haptoglobin With the Degree of Hematologic Toxicities

The levels of haptoglobin in plasma or serum samples obtained from 305 patients with advanced pancreatic cancer before gemcitabine treatment were measured by immunonephelometry and compared with the occurrence and severity of hematologic AEs. Consistent with 2DICAL analysis, the plasma levels of haptoglobin were significantly lower in the 25 patients with severe AEs than in the 22 patients without AEs ($P = .0002$, Wilcoxon test; Table 1).

The plasma level of haptoglobin showed a significant correlation with the NCI-CTCAE grade of neutropenia ($P = .012$, Kruskal-Wallis test) and hematologic toxicity categories ($P = .001$) in the 166 patients of cohort M0 (Fig 3A and Appendix Table A1). The correlation of haptoglobin levels with the grades of neutropenia and thrombocytopenia as well as the toxicity categories was consistently observed in the

Table 1. Clinical and Laboratory Data of Patients Without AEs and With Severe AEs

Factor	Patients Without AEs (n = 22)	Patients With Severe AEs (n = 25)	P
Haptoglobin, mg/dL			.0002
Mean	286	155	
SD	130	59	
Haptoglobin phenotype, No. of patients			.705*
Hp 2-2	12	14	
Hp 2-1	8	7	
Hp 1-1	2	4	
Sex, No. of patients			.344*
Male	12	17	
Female	10	8	
Age, years			.616
Mean	64	63	
SD	8	8	
ECOG performance status, No. of patients			.862*
0	12	13	
1	10	12	
2	0	0	
Body-surface area, m^2			.733
Mean	1.51	1.53	
SD	0.20	0.18	
Prior therapy, No. of patients			.867*
None	19	22	
Chemoradiotherapy using FU for LAPC	3	3	
Leucocyte, $\times 10^3/\mu L$			0002
Mean	7.4	4.8	
SD	2.8	1.4	
Absolute neutrophil count, $\times 10^3/\mu L$			.0002
Mean	5.3	3.0	
SD	2.4	1.1	
Platelet, $\times 10^4/\mu L$			< .0001
Mean	28	17	
SD	11	6	
Hemoglobin, g/dL			.806
Mean	12.1	11.9	
SD	1.4	1.4	
Albumin, g/dL			.131
Mean	3.6	3.7	
SD	0.4	0.3	
Creatinine, mg/dL			.931
Mean	0.72	0.70	
SD	0.25	0.17	
AST, U/L			430
Mean	37	29	
SD	26	13	
ALT, U/L			.624
Mean	43	32	
SD	37	24	
ALP, U/L			815
Mean	593	459	
SD	591	283	
Pharmacokinetic parameters of gemcitabine			
C_{max}, μg/mL			.594
Mean	24.02	23.21	
SD	7.18	6.68	
AUC, h · μg/mL			.462
Mean	9.95	10.74	
SD	2.36	3.03	

NOTE. Kruskal-Wallis test was applied to assess differences of values.
Abbreviations: AE, adverse event; SD, standard deviation; ECOG, Eastern Cooperative Oncology Group; FU, fluorouracil; LAPC, locally advanced pancreatic cancer; ALP, alkaline phosphatase; C_{max}, peak concentration; AUC, area under the curve.
*Calculated using the χ^2 test.

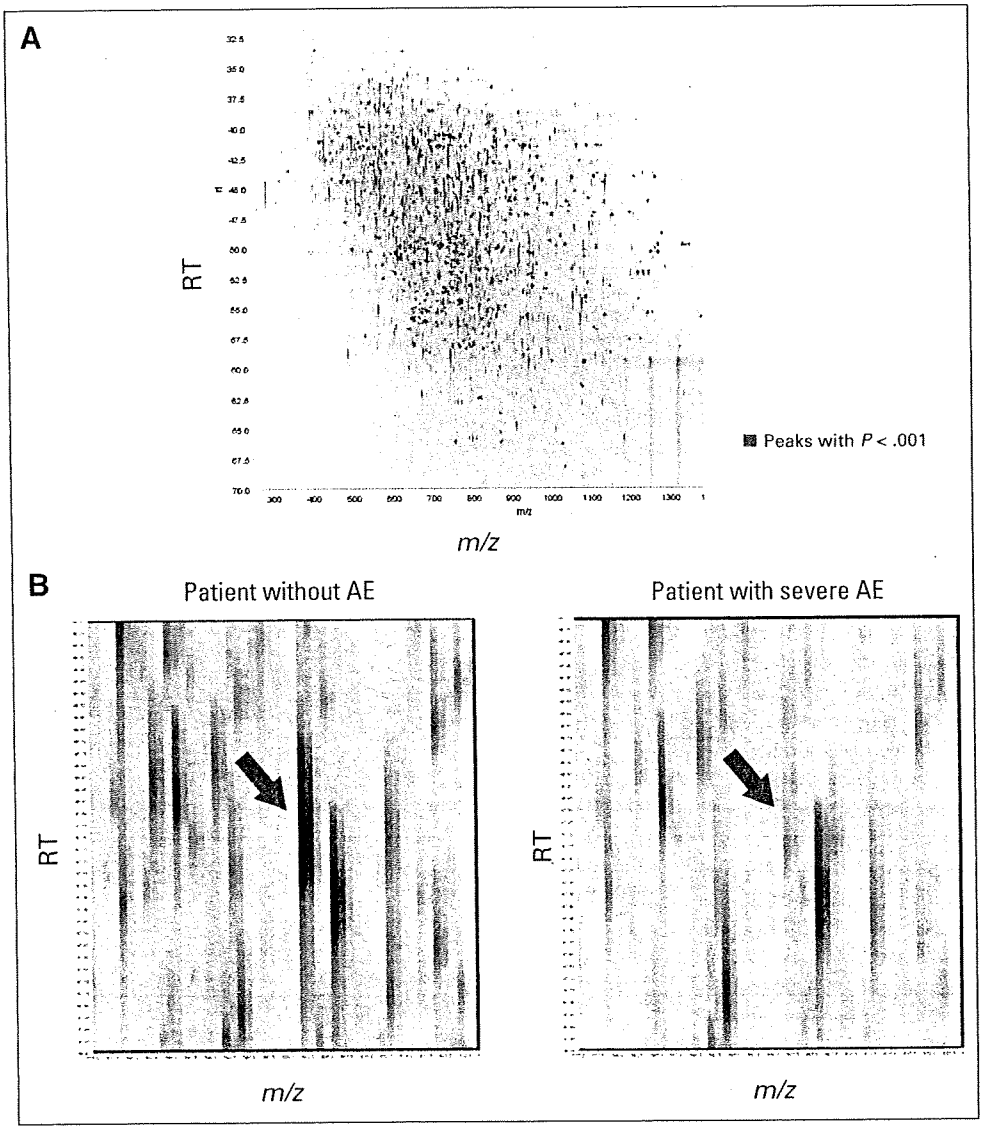

Fig 1. (A) Two-dimensional display of the entire (> 60,000) mass spectrometry (MS) peaks. The 757 MS peaks whose mean intensity differed significantly between patients with severe adverse events (AEs) and patients without AEs ($P < .001$, Welch t test) are highlighted in red. (B) MS peak with the smallest P value ($P = .0000282$; red arrows) in representative patients with severe AEs (right) and without AEs (left). RT, retention time.

two independent validation cohorts V1 (Fig 3B and Appendix Table A2) and V2 (Fig 3C and Appendix Table A3). The correlations between the levels of haptoglobin and the toxicity categories showed the highest statistical significance in all three cohorts (Figs 3A to 3C). The toxicity categories are criteria that we devised to evaluate the clinical severity of overall hematologic toxicities with emphasis on thrombocytopenia (Appendix Fig A1) from a practical viewpoint.[26-28] The management of neutropenia is largely uncomplicated because of the availability of granulocyte colony-stimulating factor.

Haptoglobin Phenotype and Hematologic Toxicities

Haptoglobin is a plasma protein that binds free hemoglobin and inhibits its oxidative activity. The human *HP* gene has two common polymorphic alleles (*H1* and *H2*), yielding individuals with the following three distinct phenotypes in the α-chain of haptoglobin protein: Hp 1-1, Hp 2-1, and Hp 2-2. The *H2* genotype has been reported to be associated with an increased risk of myocardial infarction and juvenile diabetes.[29] Although the frequency of the three phenotypes did not differ significantly with the severity of hematologic toxicities ($P > .360$, χ^2 test; Table 1 and Appendix Tables A1 to A3), the levels of haptoglobin were lower in individuals with the Hp 2-2 phenotype than in those with the Hp 2-1 or Hp 1-1 phenotype (Appendix Fig A3, online only).

Construction and Validation of a Model Predicting Hematologic Toxicities

In the M0 cohort (n = 166), 68 patients (41%) experienced category III hematologic toxicities, and 18 patients (11%) experienced category IV hematologic toxicities. Such levels of AE often necessitate the postponement of chemotherapy, and therefore, their prediction before drug administration is desirable. Because none of the parameters, including haptoglobin, was able to predict AEs satisfactorily when used individually (data not shown), we attempted to construct a multivariate predictive model to estimate the relative risk of suffering from hematologic toxicities of category III or worse. We searched for these parameters using a forward stepwise selection procedure by AIC

